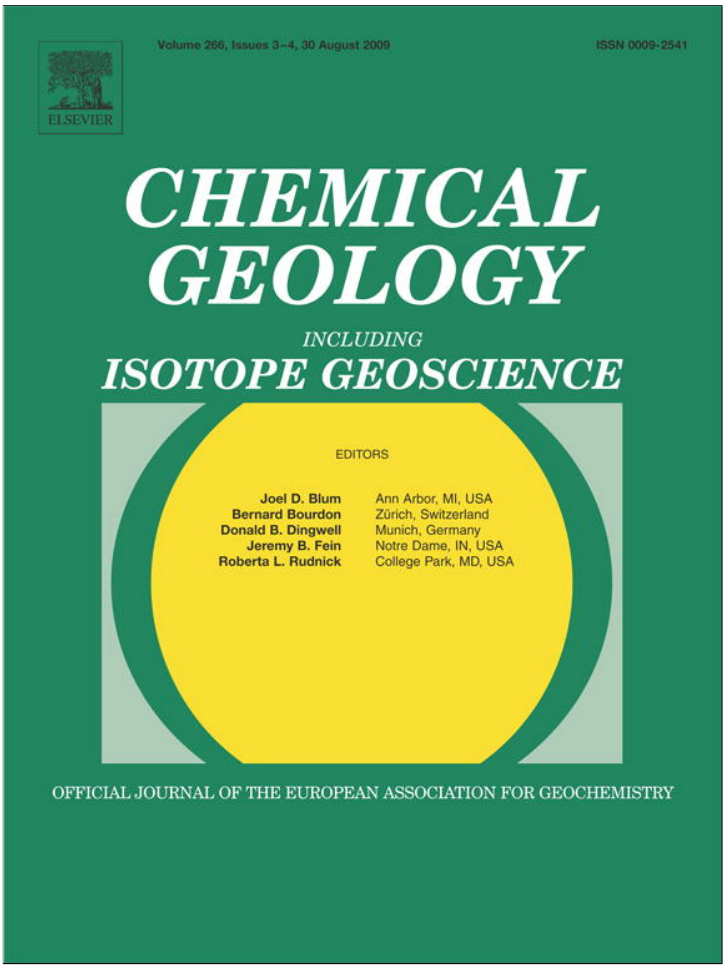

Chemical Geology 266 (2009) 359–372

Contents lists available at ScienceDirect

Chemical Geology

journal homepage: www.elsevier.com/locate/chemgeo

Origin of light volatile hydrocarbon gases in mud volcano fluids, Gulf of Cadiz — Evidence for multiple sources and transport mechanisms in active sedimentary wedges

Marianne Nuzzo [a,*], Edward R.C. Hornibrook [a], Fiona Gill [b], Christian Hensen [c], Richard D. Pancost [b], Matthias Haeckel [c], Anja Reitz [c], Florian Scholz [c], Vitor H. Magalhães [d,e], Warner Brückmann [c], Luis M. Pinheiro [e]

[a] Bristol Biogeochemistry Research Centre, Department of Earth Sciences, University of Bristol, Wills Memorial Building, Queen's Road, Bristol BS8 1RJ, United Kingdom
[b] Bristol Biogeochemistry Research Centre, Organic Geochemistry Unit, School of Chemistry, University of Bristol, Cantock's Close, Bristol BS8 1TS, United Kingdom
[c] Leibniz-Institute for Marine Sciences, IFM-Geomar, University of Kiel, East Shore Campus, Wischhofstrasse 1-3, D-24148 Kiel, Germany
[d] INETI, Marine Geology Department, Estrada do Zambujal, 2760-866 Amadora, Portugal
[e] CESAM and Geosciences Department, Universidade de Aveiro, Campus Universitário de Santiago, 3810-193 Aveiro, Portugal

ARTICLE INFO

Article history:
Received 9 October 2008
Received in revised form 29 June 2009
Accepted 30 June 2009

Editor: R.L. Rudnick

Keywords:
Mud volcanoes
Light volatile hydrocarbon gases
Migration
Unconventional methane
Lipid biomarkers

ABSTRACT

Widespread mud volcanism across the thick (≤14 km) seismically active sedimentary prism of the Gulf of Cadiz is driven by tectonic activity along extensive strike–slip faults and thrusts associated with the accommodation of the Africa–Eurasia convergence and building of the Arc of Gibraltar, respectively. An investigation of eleven active sites located on the Moroccan Margin and in deeper waters across the wedge showed that light volatile hydrocarbon gases vented at the mud volcanoes (MVs) have distinct, mainly thermogenic, origins. Gases of higher and lower thermal maturities are mixed at Ginsburg and Mercator MVs on the Moroccan Margin, probably because high maturity gases that are trapped beneath evaporite deposits are transported upwards at the MVs and mixed with shallower, less mature, thermogenic gases during migration. At all other sites except for the westernmost Porto MV, $\delta^{13}C$–CH_4 and $\delta^{2}H$–CH_4 values of ~−50‰ and −200‰, respectively, suggest a common origin for methane; however, the ratio of $CH_4/(C_2H_6+C_3H_8)$ varies from ~10 to >7000 between sites. Mixing of shallow biogenic and deep thermogenic gases cannot account for the observed compositions which instead result mainly from extensive migration of thermogenic gases in the deeply-buried sediments, possibly associated with biodegradation of C_{2+} homologues and secondary methane production at Captain Arutyunov and Carlos Ribeiro MVs. At the deep-water Bonjardim, Olenin and Carlos Ribeiro MVs, generation of C_{2+}-enriched gases is probably promoted by high heat flux anomalies which have been measured in the western area of the wedge. At Porto MV, gases are highly enriched in CH_4 having $\delta^{13}C$–CH_4 ~−50‰, as at most sites, but markedly lower $\delta^{2}H$–CH_4 values <−250‰, suggesting that it is not generated by thermal cracking of *n*-alkanes but rather that it has a deep Archaeal origin. The presence of petroleum-type hydrocarbons is consistent with a thermogenic origin, and at sites where CH_4 is predominant support the suggestion that gases have experienced extensive transport during which they mobilized oil from sediments ~2–4 km deep. These fluids then migrate into shallower, thermally immature muds, driving their mobilization and extrusion at the seafloor. At Porto MV, the limited presence of petroleum in mud breccia sediments further supports the hypothesis of a predominantly deep microbial origin of CH_4.

1. Introduction

Sub-marine mud volcanoes (MVs) provide an important pathway for the expulsion of fluids and light volatile hydrocarbon gases from dewatering sedimentary wedges in collisional settings or subduction zones (e.g., Milkov, 2005). Generation and expansion of hydrocarbon gases due to depressurization during transport is thought to constitute a major driving factor in sustaining the buoyant ascension of fluidized mud and clasts (i.e., mud breccia) and its breaching to the

* Corresponding author. Now at Leibniz-Institute for Marine Sciences, IFM-Geomar, University of Kiel, East Shore Campus, Wischhofstrasse 1-3, D-24148 Kiel, Germany. Tel.: +49 431 6002567; fax: +49 431 431 6002916.
E-mail addresses: mnuzzo@ifm-geomar.de (M. Nuzzo), Ed.Hornibrook@bristol.ac.uk (E.R.C. Hornibrook), chflg@bristol.ac.uk (F. Gill), chensen@ifm-geomar.de (C. Hensen), R.D.Pancost@bristol.ac.uk (R.D. Pancost), mhaeckel@ifm-geomar.de (M. Haeckel), areitz@ifm-geomar.de (A. Reitz), fscholz@ifm-geomar.de (F. Scholz), vhm@ua.pt (V.H. Magalhães), wbrueckmann@ifm-geomar.de (W. Brückmann), lmp@geo.ua.pt (L.M. Pinheiro).

0009-2541/$ – see front matter © 2009 Elsevier B.V. All rights reserved.
doi:10.1016/j.chemgeo.2009.06.023

seafloor (e.g., Hedberg, 1974; Brown, 1990). In spite of their key role in cold seep processes, investigations into the origins of light volatile hydrocarbon gases in such environments (Charlou et al., 2003; Blinova et al., 2003; Schmidt et al., 2005; Stadnitskaia et al, 2006; Mastalerz et al., 2007) rely almost entirely on the analysis of their molecular and stable isotopic compositions. Although models based on these parameters provide broad constraints for the formation of sedimentary hydrocarbon gases (Bernard et al., 1978; Schoell, 1980; Whiticar et al., 1986; Chung et al., 1988), major uncertainties remain for a wide range of environmental conditions (e.g., production by methanogenic *Archaea*, Valentine et al., 2004 and references therein; abiogenic generation, McCollom and Seewald, 2006; Horita and Berndt, 1999) and with regard to the effects of transport (Fuex, 1980; Prinzhofer and Pernaton, 1997). At cold seeps, these uncertainties are exacerbated by the fact that hydrocarbon gases vented at the seafloor or in the shallow subsurface may have experienced post-generational alteration during migration (e.g., James and Burns, 1984). Previous investigations of Gulf of Cadiz MVs have reported on the deep thermal origin of the light volatile hydrocarbon gases vented in this cold seep province (Mazurenko et al., 2002, 2003; Stadnitskaia et al., 2006; Hensen et al., 2007), and studies on lipid biomarkers and microbial activity at three MVs showed the occurrence of seep-related anaerobic oxidation of methane (AOM) in the past and present (Niemann et al., 2006; Stadnitskaia et al., 2008). In this study, we evaluate the conclusions of previous efforts by combining analyses of the molecular and isotopic composition of hydrocarbon gases with the organic geochemistry of the sediments to infer the depth of formation of hydrocarbon gases compared to that of fluids (Hensen et al., 2007) and of mobilized mud. Our approach shows that multiple gas sources and transport pathways occur in different areas of the tectonically active sedimentary wedge.

2. Sampling and methods

2.1. Sediment sampling

Sediment, fluid, and gas samples were recovered by gravity coring from eleven active MVs throughout the Gulf of Cadiz during the *RV-Sonne* SO 175-2 cruise in 2003 (Kopf et al., 2004), the *RV-Merian* MSM1 cruise in 2006 and the *RV-Professor Logachev* TTR-14, -15 and -16 cruises in 2004, 2005 and 2006, respectively. The sites sampled during the different expeditions are presented in Table 1 and shown in Fig. 1. The cores were segmented into 1 m lengths and cut lengthwise in a cooled laboratory at ~6 °C (except onboard the *RV-Professor Logachev*). Sediment samples were collected within 1–2 h after core retrieval. Gas hydrate samples were obtained from Porto, Captain Arutyunov and Bonjardim MVs (Table 1).

2.2. Light volatile hydrocarbon gases

Light hydrocarbon gases were stripped from mud samples onboard according to the headspace equilibration method of McAullife (1971) modified as described in Bowes and Hornibrook (2006). The gas samples were stored by displacement in glass vials filled initially with pH = 1, 10% KCl solution to avoid air contamination and microbial alteration. Concentrations of light volatile hydrocarbon gases were

Table 1
Site location, water depth and core identification for the mud volcanoes sampled in this study.

Site	Core ID	Core type	Longitude (°W)	Latitude (°N)	Water depth (m)	Core length (cmbsf)	Gas hydrate	Cruise
Bonjardim MV	GeoB9051	Gravity core	09°00.03′	35°27.61′	3087	250	Inferred	SO-175-2
	MSM1-130	Gravity core	09°00.14′	35°27.81′	3048	280		MSM1
	AT624	Gravity core	08°59.84′	35°27.56′	3065	205	Recovered	TTR-16
Carlos Ribeiro MV	MSM1-154	Gravity core	8°25.35′	35°47.26′	2198	210	–	MSM1
	AT613	Gravity core	8°25.24′	35°47.26′	2204	251	–	TTR-16
	AT614	Gravity core	8°25.30′	35°47.25′	2210	85	–	TTR-16
	AT616	Gravity core	8°25.30′	35°47.25′	2200	167	Inferred	TTR-16
Olenin MV	AT626	Gravity core	8°37.54′	35°35.00′	2628	470	No	TTR-16
Soloviev MV	AT619	Gravity core	9°06.45′	35°12.78	3295	117	Inferred	TTR-16
Semenovitch MV	AT592	Gravity core	9°05.24′	35°13.42′	3242	205	–	TTR-15
	AT620	Gravity core	9°05.20′	35°13.43′	3243	143	Inferred	TTR-16
Porto MV	AT596	Gravity core	9°30.53′	35°33.81	3878	165	Inferred	TTR-15
	MSM1-143	Gravity core	09°30.44′	35°33.70′	3862	115		MSM1
	MSM1-163	Gravity core	09°30.483′	35°33.734′	3861	–	Recovered	MSM1
	AT621	Gravity core	9°30.40′	35°33.78′	3921	140	–	TTR-16
	AT623	Gravity core	9°30.46′	35°33.76′	3875	150	Inferred	TTR-16
Captain Arutyunov MV (CAMV)	GeoB9041	Gravity core	7°19.97′	35°39.70′	1313	200	Small crystals observed	SO-175-2
	GeoB9072	Gravity core	7°19.95′	35°39.71′	1321	325	Small crystals observed	SO-175-2
	GeoB9036	TV-Grab	7°19.96′	35°29.68′	1320	–	Recovered	SO-175-2
	AT543	Gravity core	7°19.98′	35°39.69′	1345	160	Small crystals observed	TTR-14
	AT545	Gravity core	7°20.06′	35°39.69′	1337	300	Small crystals observed	TTR-14
	AT548	Kasten core	7°20.03′	35°39.70′	1345	150	Small crystals observed	TTR-14
	MSM1-205	Gravity core	7°20.08′	35°39.69′	1326	350		MSM1
	MSM1-174	Gravity core	7°19.95′	35°39.73′	1323	305		MSM1
	MSM1-218	Box core	07°20.01′	35°39.69′	1318		Recovered	MSM1
Ginsburg MV	GeoB9061	Gravity core	7°05.29′	35°22.42′	911	110	Small crystals observed	SO-175-2
	AT521	Gravity core	7°05.28′	35°22.28′	919	216	Small crystals observed	TTR-14
	AT522	Gravity core	7°05.30′	35°22.42′	912	202	–	TTR-14
Mercator MV	MSM1-239	Gravity core	6°38.70′	35°17.91′	353	200	–	MSM1
	MSM1-263	Gravity core	6°38.79′	35°17.86′	351	135	–	MSM1
Meknes MV	AT540	Gravity core	7°04.41′	34°59.07′	701	115	–	TTR-14
	AT542	Gravity core	7°04.36′	34°59.18′	703	90	–	TTR-14
	AT580	Gravity core	7°04.35′	34°59.20′	705	72	–	TTR-15
Shouen MV	AT612	Gravity core	7°15.47′	35°28.45′	1180	132	–	TTR-16

SO-175-2: *RV-Sonne* cruise SO175-2.
MSM1: *RV-Merian* cruise MSM1.
TTR-14, 15, 16: *RV-Professor Logatchev* cruises TTR-14, 15, and 16.

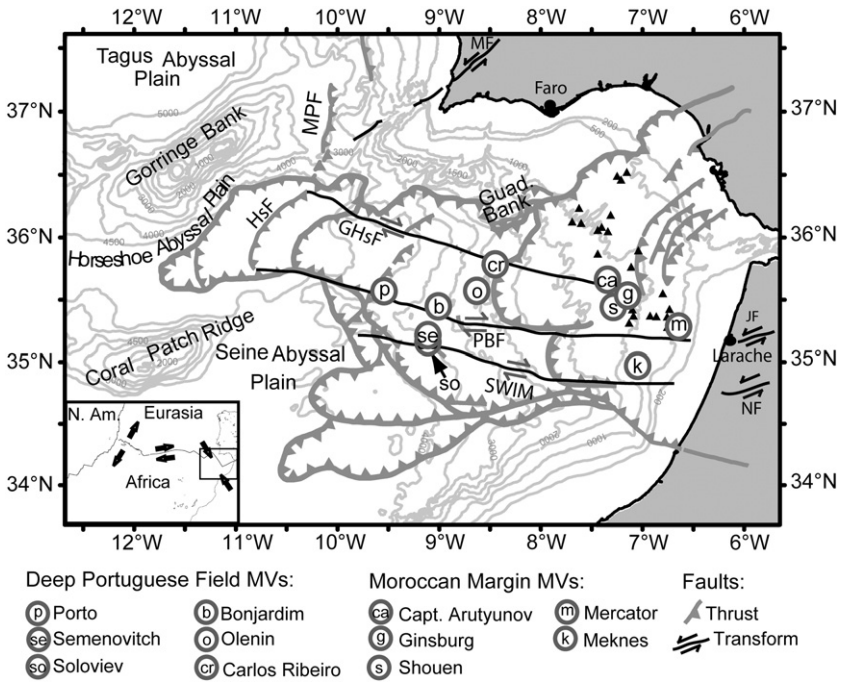

Fig. 1. Simplified structural map of the Gulf of Cadiz [modified from Medialdea et al. (2004) and Zitellini et al. (2009)], showing the contours of the sedimentary prism (in grey). Major tectonic features include (i) thrust faults of the Marquês de Pombal (MPF), and the Horseshoe (HsF), (ii) strike–slip faults of the Porto–Bonjardim (PBF), Gorringe-Horseshoe (GHsF) and SWIM shown in dark grey, and (iii) important crustal highs (Gorringe Bank, Guadalquivir Bank, and Coral Patch Ridge). Major faults onshore SW Iberia (e.g., Messejana Fault), and NW Morocco (Jebha and Nekor Faults; JF and NF, respectively) are also depicted on this Figure. The location of mud volcanoes (MVs) discovered to date is indicated by small black triangles, the 11 sites studied in this work being highlighted by white circles.

measured at the Biogeochemistry Research Centre at the University of Bristol using a Perkin Elmer Clarus 500 gas chromatograph (GC) fitted with a mega-bore PLOT Q capillary column (0.53 mm × 25 m) and on a Varian 3400 GC fitted with a PLOT Q capillary column (0.32 mm × 30 m), both equipped with a flame ionisation detector (FID) and operated with helium (35 ml min^{-1}) as carrier gas. The relative precision of the Varian 3400 was typically better than ±7% for CH_4 and C_2H_6, and ±10% for heavier homologues. The relative precision of analysis using the PE Clarus 500 instrument was better than ±2% for CH_4 and C_2H_6, and ±5% for heavier homologues. Calibration standards for methane consisted of a range of BOC (UK) alpha-gravimetric mixtures.

Analyses of $^{13}C/^{12}C$ ratios in CH_4 were conducted by GC-Combustion-Isotope Ratio Mass Spectrometry (GC-C-IRMS) at the BBRC at Bristol University using a Thermoelectron XP mass spectrometer. Light hydrocarbon gases were separated on a Varian 3400 GC fitted with a PLOT Q capillary column (0.32 mm × 30 m) and combusted to CO_2 at 1000 °C in a ceramic reactor containing Cu and Pt wires. A high purity blend of 1% O_2 in helium was fed into the reactor at 0.2 ml min^{-1} to ensure complete combustion. Analysis of $^{13}C/^{12}C$ ratios in methane homologues (ethane to pentanes) was achieved using the same instrument after GC separation of the compounds by applying the following program: online injection on port maintained at a constant temperature of 250 °C, column temperature ramping from 30 to 180 °C at a rate of 10 °C min^{-1}, and then 4 min isothermal. CH_4 calibration standards consisted of BOC (UK) alpha-gravimetric gas mixtures that had been analyzed for $\delta^{13}C$ values at external laboratories, and the values are reported in units of per mil relative to the Vienna Pee Dee Belemnite standard (‰VPDB). A $\delta^{13}C$–CO_2 gas standard was obtained from Oztech Corporation (USA), and the natural gas standard was supplied by Intergas (UK). The analytical precision of the IRMS instrument was better than ±0.5‰VPDB for CH_4 and better than ±1.5‰VPDB for C_2H_6 to C_5H_{12} homologues.

Stable isotope notation is based upon the IUPAC Recommendations 2008 document (Coplen, 2008). The delta value ($\delta^{13}C$) is defined as:

$$\delta^{13}C = \frac{(^{13}C/^{12}C)_{sample}}{(^{13}C/^{12}C)_{VPDB}} - 1 \quad (1)$$

where $(^{13}C/^{12}C)_{VPDB} = 1123.75 \times 10^{-5}$.

The stable hydrogen isotope composition of methane (δ^2H–CH_4) was analyzed on headspace gas samples at Isotech Laboratories (Champaign IL, USA) using online gas chromatography-pyrolysis-isotope ratio mass spectrometry (GC-py-IRMS). The analytical system consisted of an Agilent 6890 gas chromatograph coupled to a pyrolysis unit, Finnigan GCCIII interface, and a Thermo Delta V Plus Isotope Ratio mass spectrometer. The hydrocarbon components were separated by GC, and CH_4 was thermally converted to CO_2 and H_2 in the pyrolysis furnace at 1450 °C. The resulting H_2 was introduced directly into the mass spectrometer. The δ^2H values are reported in units of permil (‰) relative to the Vienna Standard Mean Ocean Water (VSMOW). One gas standard was analyzed every ten analyses and the analytical precision of the instrument was ±5‰VSMOW.

2.3. Sedimentary lipids

Mud breccia sediments for lipid biomarker analyses were stored at −20 °C immediately after sampling. The samples were freeze-dried at −40 °C and then extracted using a Soxhlet apparatus and a 2:1 (v:v) dichloromethane (DCM):methanol mixture for 20 h. Ten microliters of an internal standard consisting of 202 ng μl^{-1} of *n*-C_{37} and 200 ng μl^{-1} of hexadecan-2-ol was added to the samples. The organic extracts were separated by alumina gel flash column chromatography into an apolar (saturated hydrocarbon) fraction eluted with 9:1 *n*-hexane:DCM and a polar fraction (methanol). The apolar fraction was analyzed by gas chromatography using a Carlo Erba GC equipped

with a flame ionisation detector and fitted with a chrompack® fused silica capillary column (50 m × 0.32 mm internal diameter) coated with CP Sil-5CB stationary phase (dimethylpolysiloxane equivalent, 0.12 μm film thickness). The carrier gas was H_2, and the samples were injected on column using the following temperature program: 70–130 °C at 20 °C min^{-1}, 130–300 °C at 4 °C min^{-1}, and 20 min isothermal. Compound identification was performed by gas chromatography-mass spectrometry (GC-MS) on a Thermoquest Finnigan Trace GC interfaced with a Thermoquest Finnigan Trace MS operating with an electron ionisation source at 70 eV and fitted with a CP Sil-5CB column and GC conditions identical to those described above (except with He as the carrier gas). The MS was set to scan for m/z ranges of 50–850 Da.

3. Geological setting

The Gulf of Cadiz is located in a tectonically (Gràcia et al., 2003a,b) and seismically (Buforn et al., 1995) active convergent setting in which the boundary between the African and Eurasian plates is concealed beneath thick (up to ~14 km) Mio-Pliocene sedimentary deposits (Thiebot and Gutscher, 2006). The sedimentary wedge is extensively faulted (e.g., Pinheiro et al., 2003, 2005), with a predominance of conjugate NE–SW and NW–SE thrusts on the Iberian margin, and major WNW–ESE strike–slip faults, which are thought to accommodate the NW-directed plate convergence (Argus et al., 1989; Medialdea et al., 2004; Zitellini et al., 2009; Fig. 1) in a diffuse plate boundary setting (Sartori et al., 1994). Although several studies suggest that the westward progression of the Arc of Gibraltar in the Gulf of Cadiz ceased before the Pliocene (e.g., Lonergan and White, 1997), Gutscher et al. (2002) propose that E–W subduction remains active and is driven by the roll-back of a relic of subducted Tethyan oceanic crust beneath the Arc of Gibraltar.

Mud volcanism is a widespread manifestation of present-day expulsion of fluid and hydrocarbon gases from the dewatering sedimentary wedge. The MVs are mainly located along major strike–slip faults, or at the intersection of these faults with arcuate thrusts, indicating that venting occurs under tectonic control (Pinheiro et al., 2003, 2005; Fig. 1). Extensive fields of authigenic carbonate chimneys and crusts found along diapiric ridges on the Spanish and Moroccan margins indicate that intense venting of hydrocarbon gas-rich fluids has also occurred under tectonic control in the past (Diaz-del-Rio et al., 2003). Present day seepage activity in the Gulf of Cadiz has been characterized as moderate in comparison to other marine settings based on a microbiological and biogeochemical study of anaerobic

Table 2
Pore water concentrations of light volatile hydrocarbon gases in Gulf of Cadiz mud volcano sediments.

Site	Depth (cmbsf)	CH_4 (mM)§	C_2H_6 (mM)§	C_3H_8 (mM)§	i-C_4H_{10} (mM)§	n-C_4H_{10} (mM)§	i-C_5H_{12} (mM)§	n-C_5H_{12} (mM)§	$CH_4/(C_2H_6+C_3H_8)$
Bonjardim MV									
AT624	191	24.5	0.3	$2.5\ 10^{-2}$	$3.6\ 10^{-2}$	$4.7\ 10^{-3}$	0.1	$9.0\ 10^{-7}$	67
GeoB9051	240	4.1	0.3	0.1	$3.1\ 10^{-2}$	$2.4\ 10^{-2}$	$4.8\ 10^{-2}$	$7.0\ 10^{-3}$	11
MSM1-130	280	1.9	$9.9\ 10^{-2}$	$1.7\ 10^{-2}$	$4.4\ 10^{-2}$	$1.4\ 10^{-2}$	$4.4\ 10^{-2}$	$7.7\ 10^{-4}$	16
AT624 (gas hydrate)*	–	55.1	2.68	$1\ 10^{-2}$	$5\ 10^{-2}$	n.d.	n.d.	n.d.	20
Carlos Ribeiro MV									
MSM1-154	210	3.4	$4.7\ 10^{-2}$	$8.9\ 10^{-3}$	$4.2\ 10^{-3}$	$7.9\ 10^{-3}$	$7.4\ 10^{-3}$	n.d.	61
AT616	148	14.1	0.3	$5.0\ 10^{-2}$	$1.6\ 10^{-2}$	$3.9\ 10^{-2}$	$4.2\ 10^{-2}$	$1.7\ 10^{-2}$	36
AT614	84	7.8	0.2	$3.0\ 10^{-2}$	$2.7\ 10^{-2}$	$2.0\ 10^{-2}$	$2.2\ 10^{-2}$	$5.9\ 10^{-3}$	42
AT613	223	7.5	$5.8\ 10^{-2}$	$3.7\ 10^{-2}$	$1.9\ 10^{-2}$	$5.0\ 10^{-3}$	$1.1\ 10^{-2}$	$3.5\ 10^{-3}$	79
Olenin MV									
AT626	409	0.1	$5.1\ 10^{-2}$	$2.8\ 10^{-3}$	$1.5\ 10^{-3}$	$1.7\ 10^{-3}$	$6\ 10^{-4}$	$1.4\ 10^{-3}$	13
Soloviev MV									
AT619	106	8.5	$1.3\ 10^{-3}$	n.d.	n.d.	$2.9\ 10^{-4}$	n.d.	$2.1\ 10^{-4}$	6662
Semenovitch MV									
AT592	205	0.5	$1.2\ 10^{-4}$	n.d.	n.d.	n.d.	n.d.	n.d.	4536
AT620	134	11.6	$5.1\ 10^{-3}$	n.d.	$3.3\ 10^{-3}$	$4.9\ 10^{-4}$	$3.2\ 10^{-3}$	$3.4\ 10^{-4}$	2282
Porto MV									
AT596	165	5.2	$2.7\ 10^{-3}$	n.d.	n.d.	n.d.	n.d.	n.d.	1908
AT621	129	8.6	$1.1\ 10^{-3}$	n.d.	n.d.	n.d.	n.d.	n.d.	7660
AT623	150	21.7	$9.4\ 10^{-3}$	n.d.	n.d.	n.d.	n.d.	n.d.	2298
MSM1-143	102	3.5	$6.8\ 10^{-4}$	n.d.	n.d.	$8.4\ 10^{-5}$	n.d.	n.d.	5251
MSM1-163 (gas hydrate)*	–	98.1	n.d.	n.d.	n.d.	n.d.	n.d.	n.d.	1462
Captain Arutyunov MV									
GeoB9041	195	5.2	$4.0\ 10^{-3}$	$6.0\ 10^{-4}$	$1.8\ 10^{-4}$	$6.4\ 10^{-5}$	$4.5\ 10^{-5}$	$5.8\ 10^{-5}$	1109
GeoB9072	300	8.2	$3.7\ 10^{-3}$	$1.4\ 10^{-3}$	$4.7\ 10^{-4}$	$1.6\ 10^{-4}$	n.d.	n.d.	1594
MSM1-174	305	4.3	$2.1\ 10^{-3}$	$2.3\ 10^{-3}$	$8.3\ 10^{-4}$	$2.7\ 10^{-4}$	$1.1\ 10^{-3}$	n.d.	995
MSM1-205	295	2.5	$4.4\ 10^{-3}$	$1.5\ 10^{-3}$	$9.7\ 10^{-4}$	$1.8\ 10^{-4}$	$2.7\ 10^{-4}$	n.d.	429
AT545	300	4.3	$2.7\ 10^{-3}$	n.d.	n.d.	$8.4\ 10^{-4}$	n.d.	$9.7\ 10^{-4}$	1611
MSM1-218 (gas hydrate)*	–	18.2	$2.8\ 10^{-2}$	n.d.	n.d.	n.d.	n.d.	n.d.	660
GeoB9036 (gas hydrate)*	–	52.4	$6\ 10^{-2}$	$2.5\ 10^{-4}$	n.d.	n.d.	n.d.	n.d.	616
AT544 (gas hydrate)*	–	50.4	$7.4\ 10^{-2}$	$1.3\ 10^{-4}$	n.d.	n.d.	n.d.	n.d.	674
Ginsburg MV									
GeoB9061	140	4.8	$9.3\ 10^{-2}$	$2.3\ 10^{-2}$	$2.5\ 10^{-3}$	$2.2\ 10^{-2}$	$2.0\ 10^{-2}$	$1.1\ 10^{-2}$	41
AT521	175	5.6	$7.9\ 10^{-3}$	$1.1\ 10^{-3}$	n.d.	$1.0\ 10^{-3}$	n.d.	$1.1\ 10^{-3}$	628
AT522	190	2.6	$1.5\ 10^{-2}$	$6.7\ 10^{-3}$	$5.6\ 10^{-3}$	$4.5\ 10^{-3}$	n.d.	n.d.	125
Mercator MV									
MSM1-239	200	1	$6.4\ 10^{-3}$	$2.3\ 10^{-3}$	$3.6\ 10^{-3}$	$1.3\ 10^{-3}$	$8.9\ 10^{-3}$	$6.6\ 10^{-4}$	112
MSM1-263	135	1.4	$2.3\ 10^{-2}$	5.9 10	$4.3\ 10^{-3}$	$1.4\ 10^{-3}$	$2.4\ 10^{-3}$	$5.4\ 10^{-4}$	50
Meknes MV									
AT540	100	5.8	$1.2\ 10^{-2}$	$6.2\ 10^{-3}$	$1.4\ 10^{-3}$	$5.1\ 10^{-3}$	$9.0\ 10^{-4}$	$2.8\ 10^{-3}$	289
AT542	90	5.3	$1.3\ 10^{-3}$	$2.4\ 10^{-4}$	n.d.	$4.0\ 10^{-4}$	n.d.	n.d.	3390
AT580	85	0.2	$6.9\ 10^{-5}$	n.d.	n.d.	n.d.	n.d.	n.d.	2313

*Gas hydrate recovered in sediments by gravity coring, concentration values expressed in percent volume (%v).
§Calculations to obtain concentrations in mM are provided in Nuzzo (2007).

Table 3
Stable carbon and hydrogen isotope composition of methane, and stable carbon isotope composition of ethane to pentanes in pore fluids from Gulf of Cadiz mud volcanoes.

Site	Depth (cmbsf)	$\delta^{13}C$–CH_4 (‰VPDB)	(*n*)	δD-CH_4 (‰VSMOW)	$\delta^{13}C$–C_2H_6 (‰VPDB)	(*n*)	$\delta^{13}C$–C_3H_8 (‰VPDB)	(*n*)	$\delta^{13}C$-i-C_4H_{10} (‰VPDB)	(*n*)	$\delta^{13}C$-n-C_4H_{10} (‰VPDB)	(*n*)	$\delta^{13}C$-i-C_5H_{12} (‰VPDB)	(*n*)	$\delta^{13}C$-n-C_5H_{12} (‰VPDB)
Bonjardim															
AT624	112–191	−49.9 ± 0.4	8		−27.5 ± 0.3	12	−20.4 ± 0.5	4	−27.3 ± 0.5	4	−21.6	1	−24.6 ± 0.4	4	–
GeoB9051	150-240	−49.5 ± 0.2	6		−27.9 ± 0.2	7	−24.1 ± 0.5	7	−26.6 ± 0.5	7	−24.8 ± 1.2	7	−25.4 ± 0.4	7	–
MSM1-130	180–280	−49.4 ± 0.5	5		−27.3 ± 0.2	8	−21.3 ± 0.7	8	−25.9 ± 0.8	3	−25.5 ± 1.6	8	−24.0 ± 0.9	8	−24.8 (*n* = 1)
AT624 *	–	−52.7	1	−202	−27.6	1	−19.0	1	−26.0	1	−29.4	1			
Carlos Ribeiro															
MSM1-154	55–210	−54.9 ± 0.3	8	−210 (200)*	−24.2 ± 0.4	13	−22.0 ± 1.3	6	−25.2 ± 0.7	6	−28.3	1	−24.9 ± 0.1	3	−20 ± 1.2 (*n* = 3)
AT616	89–168	−54.1 ± 0.9	5	−187 (148)*	−24.0 ± 0.2	6	−22.0 ± 0.4	4	−24.8 ± 1.4	4	−24.8 ± 1.4	4	−25.0 ± 0.4	4	−26.2 ± 2.2 (*n* = 3)
AT614	64–84	−51.9 ± 1.3	3		−23.4 ± 0.2	3	−19.7	1	−24.2 ± 0.1	3	−22.4 ± 0.3	3	−25.5 ± 0.6	3	−21.3 (*n* = 1)
AT613	213–244	−69.0 ± 0.4	3		−32.8 ± 1.3	3	−17.0 ± 0.4	7	−23.5 ± 0.1	3	−20.24	1	−24.0 ± 0.6	3	n.d.
Soloviev															
AT619	106	−57.0	1	−186 (96)*	n.d.		n.d.		n.d.		n.d.		n.d.		n.d.
Semenovitch															
AT592	205	−73.3	1	−210 (205)*	n.d.		n.d.		n.d.		n.d.		n.d.		n.d.
AT620	98–134	−53.8 ± 0.5	5	−214 (134)*	n.d.		n.d.		n.d.		n.d.		n.d.		n.d.
Porto															
AT596	165	−55.6	1		n.d.		n.d.		n.d.		n.d.		n.d.		n.d.
AT621	129	−53.7	1	−257 (129)*	n.d.		n.d.		n.d.		n.d.		n.d.		n.d.
AT623	120–150	−51.7 ± 0.4	3	−262 (150)*	n.d.		n.d.		n.d.		n.d.		n.d.		n.d.
MSM1-143	72–115	−53.1 ± 0.5	5	−226 (52)*	n.d.		n.d.		n.d.		n.d.		n.d.		n.d.
MSM1-163*	–	−54.9	1	−261	n.d.		n.d.		n.d.		n.d.		n.d.		n.d.
CAMV															
GeoB9041	55–195	−48.5 ± 0.2	12	−204 (195)*	n.d.		n.d.		n.d.		n.d.		n.d.		n.d.
GeoB9072	210–325	−47.7 ± 0.2	12		n.d.		n.d.		n.d.		n.d.		n.d.		n.d.
MSM1-174	115–305	−47.9 ± 0.8	8	−182 (305)*	−24.4 ± 1.1	4	−10.7 ± 1.8	4	−24.6	1	n.d.		n.d.		n.d.
MSM1-205	70–350	−48.4 ± 1.7	10		n.d.		n.d.		n.d.		n.d.		n.d.		n.d.
AT545	100–300	−46 ± 0.4	12		n.d.		n.d.		n.d.		n.d.		n.d.		n.d.
MSM1-218*	–	−50.5	1		−25.3	1	n.d.		n.d.		n.d.		n.d.		n.d.
GeoB9036*	–	−52.0	1	−192	n.d.		n.d.		n.d.		n.d.		n.d.		n.d.
AT544*	–	−50.7	1		n.d.		n.d.		n.d.		n.d.		n.d.		n.d.
Ginsburg															
GeoB9061	73–140	−40.8 ± 0.2	8	−153 (155)*	−22.5	1	−22.1	1	−24.1	1	n.d.		n.d.		n.d.
AT521	125–175	−48.9 ± 1.4	6	−220 (313)*	n.d.		n.d.		n.d.		n.d.		n.d.		n.d.
AT522	130–190	−47.2 ± 0.2	8		n.d.		n.d.		n.d.		n.d.		n.d.		n.d.
Mercator															
MSM1-239	95–200	−33.8 ± 0.4	5	−129 (200)*	−34.1 ± 1.1	6	−17.3	1	−25.9	1	−31.1	1	−25	1	−27.3 (n = 1)
MSM1-263	70–135	−38.8 ± 0.6	4	−142 (135)*	−23.9 ± 0.2	4	−25.4 ± 0.7	4	−27.4 ± 0.5	4	−25.2	1	−27.2 ± 1.1	3	
Meknes															
AT540	50–130	−51.6 ± 0.1	9	−204 (110)*	n.d.		n.d.		n.d.		n.d.		n.d.		n.d.
AT542	70–90	−48.9 ± 0.3	3		n.d.		n.d.		n.d.		n.d.		n.d.		n.d.
AT580	85	−52.8	1		n.d.		n.d.		n.d.		n.d.		n.d.		n.d.

*The number in between brackets indicates the depth of the sample (in cmbsf).

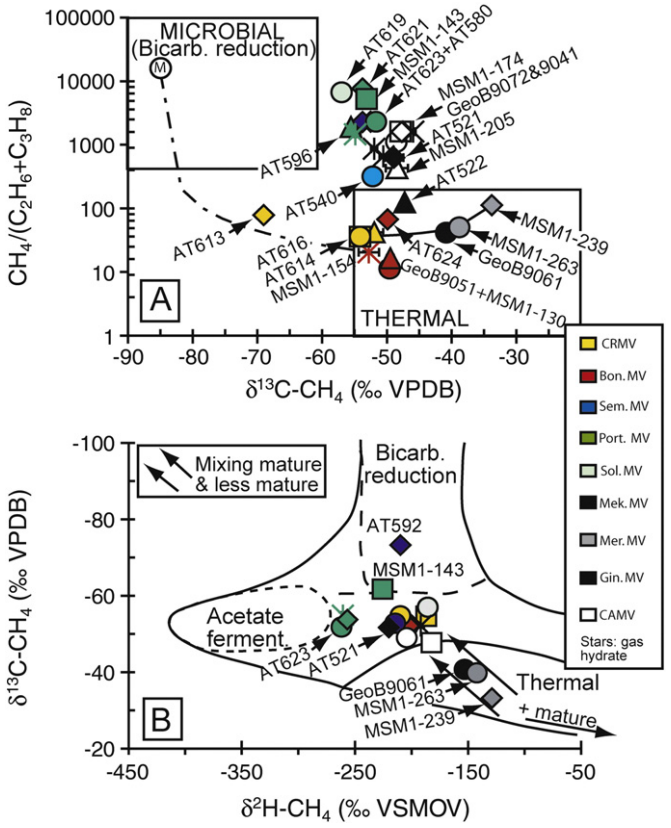

Fig. 2. [A] "Bernard diagram" plotting $\delta^{13}C$–CH_4 (in ‰VPDB) versus $CH_4/(C_2H_6+C_3H_8)$ in samples from nine Gulf of Cadiz MVs (after Bernard et al., 1978). Carlos Ribeiro MV (CRMV): circles: MSM1-154; triangles: AT614; diamonds: AT613; squares: AT616. Bonjardim MV (Bon. MV): circles: GeoB9051; triangles: MSM1-130; diamonds: AT624; star: gas hydrate (AT624). Semenovich MV (Sem. MV): circles: AT620; diamonds: AT592. Porto MV (Port. MV): circles: AT623; diamonds: AT621; triangles: AT596; squares: MSM1-143; star: gas hydrate (MSM1-163). Soloviev MV (Sol. MV): circles: AT619. Meknes MV (Mek. MV): circles: AT540; diamonds: AT580; triangles: AT542. Mercator MV (Mer. MV): circles: MSM1-268; diamonds: MSM1-239. Ginsburg MV (Gin. MV): circles: GeoB9061; diamonds: AT521; triangles: AT522. Captain Arutyunov MV (CAMV): circles: GeoB9041; diamonds: GeoB9072; triangles: MSM1-205; squares: MSM1-174; dash: AT545; cross: gas hydrate (MSM1-218); star: gas hydrate (GeoB9036). The two rectangular fields represent typical $\delta^{13}C$–CH_4 values and $CH_4/(C_2H_6+C_3H_8)$ ratios for microbial (M) and thermogenic (T) gases. The mixing curve (broken line) joining the two fields shows the improbability that the isotopic and molecular signatures of gases at all sites could result from mixing of conventional microbial and thermogenic gases, except in core AT613 from Carlos Ribeiro MV. The mixing line (plain line) between high thermal maturity gas from Mercator MV vent (MSM1-239) and lower thermal maturity gas from Carlos Ribeiro MV (e.g., MSM1-154) shows that the composition of gases at Ginsburg MV (GeoB9061) and Mercator MV (MSM1-263) could be produced by such a mixture. [B] "C-D Diagram" plotting pore water δD- versus $\delta^{13}C$–CH_4 in samples from nine Gulf of Cadiz mud volcanoes (modified after Whiticar et al., 1986). The fields correspond to combined stable hydrogen and carbon isotope compositions typical for CH_4 formed by thermal cracking of sedimentary organic matter ("Thermal"); by *Archaea*-mediated reduction of sedimentary CO_2 coupled to the oxidation of H_2 ("Bicarbonate reduction"); by *Archaea*-mediated fermentation of acetate to CO_2 and CH_4 ("Acetate fermentation").

oxidation of methane at three active MVs (Niemann et al., 2006). However, active seepage of fluids and hydrocarbon gases to the water column has been observed recently during filming of the seafloor at Mercator MV (van Rooij et al., 2005; Kenyon et al., 2005) and the presence of gas hydrates at several MVs across the Gulf of Cadiz is indicative of sustained fluxes of hydrocarbon-rich fluids at these sites.

4. Results

4.1. Light volatile hydrocarbon gases in interstitial fluids

The pore water hydrocarbon gas samples were recovered in the deepest part of the cores, well below the sulphate–methane transition zone, as shown on pore water geochemical profiles in Hensen et al. (2007) and Nuzzo et al. (2008). These samples are therefore thought to reflect the composition of deep hydrocarbon gases transported towards the seafloor at the MVs. Pore water concentrations of light volatile hydrocarbon gases (methane to pentanes) in mud breccia sediments are provided in Table 2, with carbon and hydrogen isotopic compositions listed in Table 3. Fig. 2a presents a "Bernard diagram", plotting $\delta^{13}C$–CH_4 values versus $CH_4/(C_2H_6+C_3H_8)$ ratios for pore water hydrocarbon gases (Bernard et al., 1978). Samples from Bonjardim, Carlos Ribeiro, Ginsburg and Mercator MVs are characterized by a significant abundance of higher molecular weight methane homologues with $CH_4/(C_2H_6+C_3H_8)$ ratios as low as ~10 at Bonjardim MV. The $\delta^{13}C$–CH_4 values range from ~−54‰ at Carlos Ribeiro MV to ~−35‰ at Mercator MV. In contrast, samples from all other sites (CAMV, Porto, Meknes, Semenovich, Soloviev MVs) and from core AT521 at Ginsburg MV have $\delta^{13}C$–CH_4 values of ~−50‰, but much higher and more variable proportions of CH_4 relative to heavier homologues ($290 \leq CH_4/(C_2H_6+C_3H_8) \leq 7700$). In contrast to most of the data, samples from one core at Carlos Ribeiro MV (AT613) contained more ^{13}C-depleted CH_4 (-69.0 ± 0.4‰; Table 3). Compositionally different as well was the gas from the active seafloor vent at Mercator MV (core MSM1-239) which was ^{13}C-enriched CH_4 (and had $CH_4/(C_2H_6+C_3H_8)$ ratios up to 330.

A "C-D diagram" (Whiticar et al., 1986) plotting $\delta^{13}C$- versus $\delta^{2}H$–CH_4 values for samples from 8 MVs is shown in Fig. 2b. Samples from Mercator and Ginsburg MVs on the Moroccan Margin have $\delta^{13}C$- and $\delta^{2}H$–CH_4 values ranging from −40 to −35‰ and −153 to −129‰, respectively, with the highest values analyzed at the bubbling site at Mercator MV (MSM1-239). Methane $\delta^{13}C$ and $\delta^{2}H$ values are more negative at all the other sites, including the second core from Ginsburg MV (AT521). CH_4 from Porto MV is distinctively ^{2}H-depleted compared to samples from all other sites.

The series of $\delta^{13}C$ values for the different light volatile hydrocarbon gases are plotted in order of increasing molecular weight of the homologues in Fig. 3. At most sites, the $\delta^{13}C$-values for CH_4 are markedly more negative than the homologues, which range between −30 and −20‰, typical of thermogenic gases (Chung et al., 1988). Propane, however, is clearly more ^{13}C-enriched than the other homologues at CAMV, with values as positive −8‰. An exception is the Mercator MV where CH_4 has a $\delta^{13}C$ value of ~−35‰ very similar to that of higher homologues. Samples from core AT613 at Carlos Ribeiro MV also depart from the general trends because both CH_4 and C_2H_6 possess markedly more negative $\delta^{13}C$ values whereas C_3H_8 is relatively enriched in ^{13}C (Fig. 3).

Plotting the $\delta^{13}C$–C_3H_8 values against pore water concentrations of propane (Fig. 4a) delineates three main groupings of C_3H_8 data: (i) samples from most sites having $\delta^{13}C$–C_3H_8 values of ~−21‰,

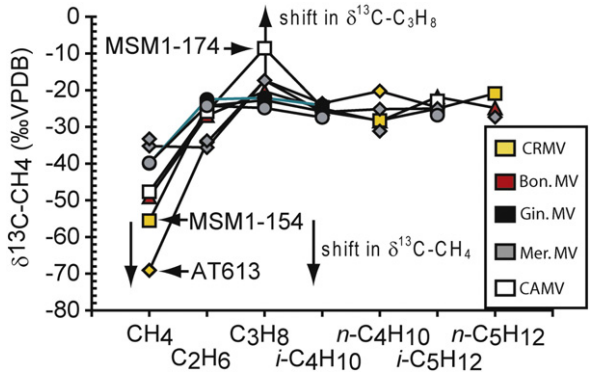

Fig. 3. Plot showing $\delta^{13}C$-values for CH_4 to C_5H_{12} homologues (‰VPDB) at Carlos Ribeiro MV; Bonjardim MV; CAMV; Ginsburg MV; and Mercator MV (adapted from Chung et al., 1988). Colour code for sites as shown on figure.

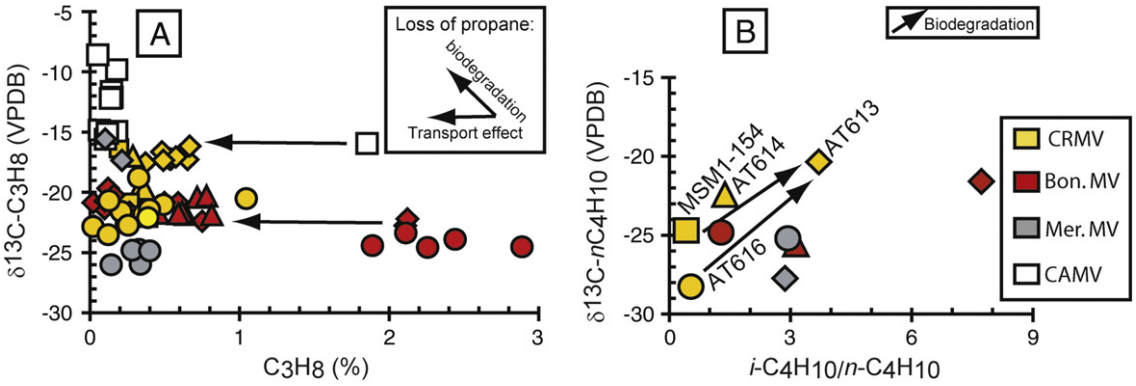

Fig. 4. [A] Diagram plotting δ^{13}C- against the concentration in propane and showing trends for transport and biodegradation effects. [B] Plot of the ratio *i*-C_4H_{10}/*n*-C_4H_{10} against δ^{13}C-*n*-C_4H_{10}. The arrow shows a trend for increasing biodegradation effect between samples from Carlos Ribeiro MV. Colour code for sites as shown on figure.

(ii) samples from core AT613 at Carlos Ribeiro MV with δ^{13}C–C_3H_8 values of −17‰, and (iii) samples from core MSM1-263 from the non-bubbling site at Mercator MV having the most ^{13}C-depleted propane (~−25‰). Overall, concentration values vary at different locations (cores) of the MVs but the isotopic compositions remain similar, with the exception of CAMV where δ^{13}C–C_3H_8 values are markedly higher (up to −8‰) and concentrations lower than at other sites.

A trend of increasing ratio of iso-C_4H_{10} to normal-C_4H_{10} with increasing δ^{13}C–*n*C_4H_{10} values is apparent for samples from cores AT616, AT614 and AT613 at Carlos Ribeiro MV and cores MSM1-130 and AT624 at Bonjardim MV (Fig. 4b). At Mercator MV, the ratio *i*-C_4H_{10}/*n*-C_4H_{10} is similar (~3) for samples from the active vent (MSM1-239) and the non-bubbling site (MSM1-263), but δ^{13}C-*n*-C_4H_{10} values are different (−31.1‰ and −25.2‰, respectively).

4.2. Lipid biomarkers

4.2.1. Acyclic alkanes

The distribution of acyclic hydrocarbons is highlighted for CAMV, Bonjardim MV and Olenin MV by the *m*/*z* 57 mass chromatogram in Fig. 5, with the distribution of all hydrocarbons shown by the total ion current (TIC) mass chromatogram in the insert. Hydrocarbons are dominated at CAMV and Bonjardim MV by *n*-alkanes ranging from C_{17} to C_{35} and the regular isoprenoids pristane and phytane, but not at Olenin MV where pristane and phytane abundances are low (Fig. 5). The distribution in *n*-alkanes follows two distinct patterns. In the first distribution pattern, the peaks corresponding to odd carbon number *n*-alkanes are higher than their even homologues in the range of C_{25} to C_{31}. The second pattern shows a clear decrease in *n*-alkane abundances with increasing carbon chain length and no odd-over-even carbon number preference (or vice versa). The first pattern prevails at Olenin MV and the second at CAMV as shown in Fig. 5 and indicated in Table 5 by the Carbon Preference Index (CPI) and the Odd Even Preference (OEP) indexes. A mixed distribution can be observed at Bonjardim MV on Fig. 5b. A similar trend is shown at all other sites by an increasing odd versus even predominance of C_{25}–C_{31} compounds from Carlos Ribeiro and Bonjardim MVs to Porto MV (core AT621; Table 5). In general, hydrocarbon abundances are lowest where the odd-numbered *n*-alkanes (C_{25} to C_{31}) dominate the distribution pattern, as shown at Olenin MV, where both the number of compounds and their amounts are lower than at other sites (Fig. 5c).

4.2.2. Hopanes

The distribution of hopanes is highlighted by the *m*/*z* 191 mass chromatograms at CAMV, Bonjardim MV and Olenin MV (Fig. 6), with the 17β,21α(H)/(17β,21α(H) + 17α,21β(H)) hopane ratio highlighted in Table 5 (hereby referred to as βα/(βα + αβ) ratio). The key to compound identification in Fig. 6 is given in Table 4. The hopane distribution is similar at all sites, marked by the coexistence of thermally immature (i.e., hopanes in their biological 17β,21β(H) stereochemical

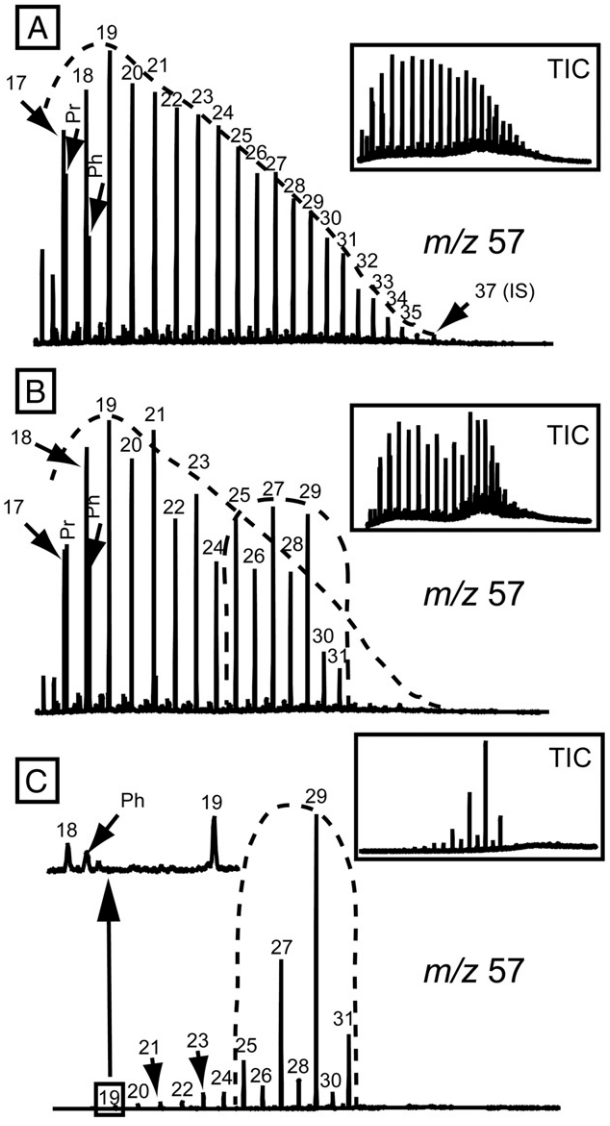

Fig. 5. Distribution of *n*-alkanes, pristane and phytane highlighted by partial *m*/*z* 57 mass chromatograms of the saturated hydrocarbons extracted from mud breccia sediments from [A] Captain Arutyunov MV (GeoB9072); [B] Bonjardim MV (AT624); and [C] Olenin MV (AT626). The distribution of all saturated hydrocarbons is shown in the partial total ion current mass chromatograms in insert for the respective sites.

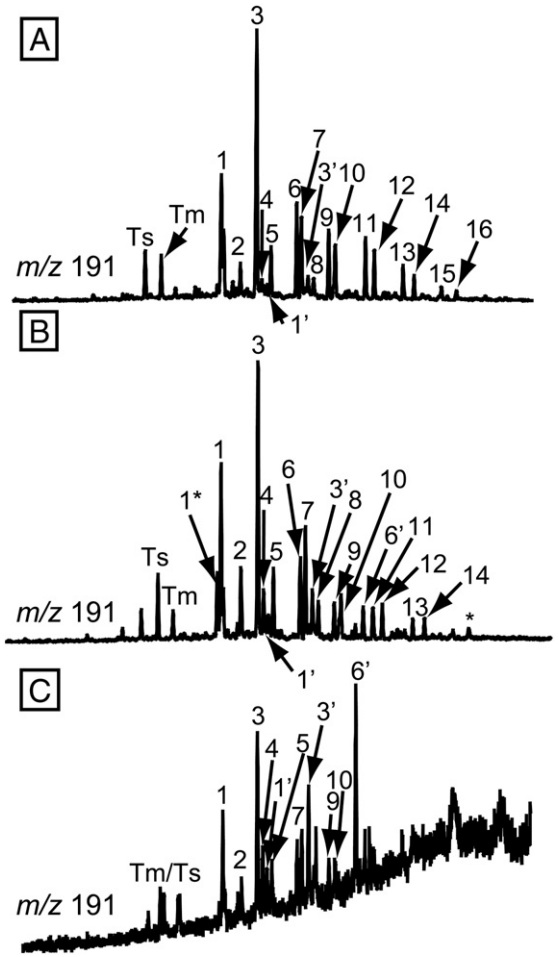

Fig. 6. Distribution of hopanes highlighted by partial *m/z* 191 mass chromatograms of the saturated hydrocarbons extracted from mud breccia sediments from [A] Captain Arutyunov MV (GeoB9072); [B] Bonjardim MV (AT624); [C] Olenin MV (AT626). Partial total ion current mass chromatograms are shown in Fig. 5. The key to compound identification is provided in Table 4.

configuration; peaks 1′, 2′ and 6′ in Fig. 6) and mature (17α,21β(H) hopanes and both 22S and 22R isomers; peaks 4, 5, 6–12 in Fig. 6) compounds. Homohopanes with the αβ configuration predominate over thermally immature hopanes at CAMV, and to a lesser extent at Carlos Ribeiro and Bonjardim MVs, whereas thermally immature hopanes are relatively more abundant at Ginsburg and Porto MVs and dominate the distribution at Olenin MV (Fig. 6 and Table 5). At Olenin MV, the predominance of immature biomarkers correlates with very low hopane abundances (Fig. 6c).

4.2.3. Steranes and diasteranes

The distribution of steranes, diasteranes and monoaromatic steranes is highlighted by the *m/z* 217 mass chromatograms for CAMV, Bonjardim MV and Olenin MV (Fig. 7), and indicated by the diasteranes/(diasteranes + steranes) and C_{21}–C_{22} monoaromatic steranes ratios in Table 5. The key to compound identification in Fig. 7 is given in Table 4. As observed for hopanes, the sterane distributions are similar at all sites, except at Olenin MV. At most sites, the distribution is dominated by C_{27} and C_{29} diasteranes and C_{27}, C_{28} and C_{29} steranes. Low molecular weight steranes (C_{21}–C_{22}) occur in highest relative abundances at CAMV, with lower relative abundances at Carlos Ribeiro MV, and very low abundances at Bonjardim, Ginsburg and Porto MVs. At Olenin MV, sterane abundances are much lower than at all other sites and C_{21}–C_{22} components were not detected (Table 5).

5. Discussion

5.1. Gases of different origins at Gulf of Cadiz mud volcanoes

At most sites, the $\delta^{13}C$ values of vented methane generally suggest a deep thermal origin (Fig. 2a), consistent with reports from Mazurenko et al. (2002, 2003), Stadnitskaia et al. (2006) and Hensen et al. (2007). Samples from core AT613 at Carlos Ribeiro MV are an exception in that the data plot along a mixing line between i) thermogenic gas having a composition similar to that observed in other Carlos Ribeiro MV cores, and ii) a microbial end-member, as depicted in Fig. 2a. Stadnitskaia et al. (2006) identified two groups of MVs across the Gulf of Cadiz based on the composition of hydrocarbon gases. These authors distinguished thermogenic gases vented at Moroccan Margin MVs, which are thought to have a higher thermal maturity based on their molecular and isotopic compositions, from gases seeping at Deep Portuguese Field (DPF) MVs, which they characterized as mainly thermogenic in origin but of a lower maturity and containing admixtures of shallow Archaeal CH_4. Our results are in agreement with those of Stadnitskaia et al. (2006) regarding the occurrence of thermogenic gases of different thermal maturities at the MVs. In contrast to Stadnitskaia et al. (2006), however, we observed that venting of lower thermal maturity gases is not restricted to the DPF MVs, but does also occur at many Moroccan Margin sites. Additionally, at Porto MV in the DPF, our results suggest that the gases do not have a main thermogenic origin. We will therefore refer to sites venting "mature" and "lower maturity" thermogenic gases instead of DPF and Moroccan Margin sites, and discuss the case of Porto MV separately.

5.1.1. "Lower maturity thermogenic gases"

Pore water gas samples from the DPF MVs have relatively invariant methane $\delta^{13}C$ values of ~ −50‰ but also highly variable $CH_4/(C_2H_6+$

Table 4
Hopane and sterane identification key for Figs. 6 and 7, respectively.

Peak number	Compound/configuration	Carbon number
Ts	22,29,30-Trisnorhopane-II	27
Tm	22,29,30-Trisnorhopane	27
1*	Hopene	29
1	17α,21β(H)-30-norhopane	29
2	17β,21α(H)-30-norhopane (normoretane)	29
3	17α,21β(H)-30-hopane	30
4	17α(H)-30-nor-29-homohopane	30
1′	17β,21β(H)-30-norhopane	29
5	17β,21α(H)-30-hopane (moretane)	30
6	17α,21β(H)-29-homohopane 22*S*	31
7	17α,21β(H)-29-homohopane 22*R*	31
3′	17β,21β (H)-30-hopane	30
8	17α,21β(H)-29-homohopane 22*S* + 22*R*	31
9	17α,21β(H)-29-bishomohopane 22*S*	32
10	17α,21β(H)-29-bishomohopane 22*R*	32
6′	17β,21β (H)-29-homohopane	31
11	17α,21β(H)-29-trishomohopane 22*S*	33
12	17α,21β(H)-29-trishomohopane 22*R*	33
13	17α,21β(H)-29-tertrakishomohopane 22*S*	34
14	17α,21β(H)-29-tertrakishomohopane 22*R*	34
15	17α,21β(H)-29-pentakishomohopane 22*S*	35
16	17α,21β(H)-29-pentakishomohopane 22*R*	35
*	Contamination (column bleed)	
a	Diasterane	27
b	Diasterane	27
c	5α,14α,17β-Cholestane	27
d	5α,14α,17-Cholestane	27
e	Diasterane	29
f	5α,14α,17-Ergostane	28
g	5α,14β,17α-Stigmastane	29
h	5α,14α,17-Stigmastane	29
i	13β,17α-dia-n-propylcholestane	30

Table 5
Maturity-dependent biomarker parameters for Gulf of Cadiz mud volcano apolar lipid extracts.

Site (core ID)	CPI	OEP_1	OEP_2	Diast./(Diast + Ster.)[a] (%)	βα/(βα + αβ) Hopanes (%)[b]	22S/(22S + 22R)[c]	MA(I)/(MA(I) + MA(II))[d]
Ginsburg MV (GeoB9061)	1.3	1.2	1.2	15.8	41.7	0.3	19.8
Shouen MV (AT612)	1.2	1.4	1.1	16.7	63.3	0.3	37.5
Carlos Ribeiro MV							
AT616	1.2	1.1	1.3	23.2	33.0	0.5	27.8
AT614	1.2	1.1	1.3	–	–	0.5	39.3
AT613	1.2	1.1	1.3	24.0	39.4	0.5	47.2
Bonjardim MV(AT624) (40–50 cmbsf)	1.3	1.2	1.2	21.7	36.5	0.4	24.4
(102–112 cmbsf)	1.3	1.2	1.2	23.1	37.3	–	46.1
(191–201 cmbsf)	1.3	1.2	1.2	20.3	25.1	0.4	15.5
Olenin MV (AT626)	4.5	1.4	3.9	–	40.3	n.d.	–
CAMV (GeoB9072)	1.1	1	1.9	26.5	31.6	0.6	50.0
Porto MV AT621	2.1	1.3	2.0	14.8	39.2	0.4	24.7
AT623 (50–60 cmbsf)	1.7	1.4	1.7	22.7	40.2	0.4	32.1
(130–140 cmbsf)	1.4	1.4	1.1	24.1	–	0.4	28.3
Semenovitch MV (AT620)	1.3	1.1	1.5	25.8	17.6	0.5	36.0
Soloviev MV (AT619)	1.3	1.3	1.2	20.7	22.0	0.4	24.8

(a) C_{27}–C_{29} diasteranes/(C_{27}–C_{29} regular steranes + C_{27}–C_{29} diasteranes).
(b) 17β,21α (H)-30-norhopane (normoretane)/17α,21β (H)-30-norhopane.
(c) 17α,21β (H)-29-Bishomohopane (22*S*)/[17α,21β (H)-29-Bishomohopane (22*S*) + 17α,21β (H)-29-Bishomohopane (22*R*)].
(d) C_{21}–C_{22} monoaromatic steroids: MA(I); C_{27}–C_{29} monoaromatic steroids: MA(II).

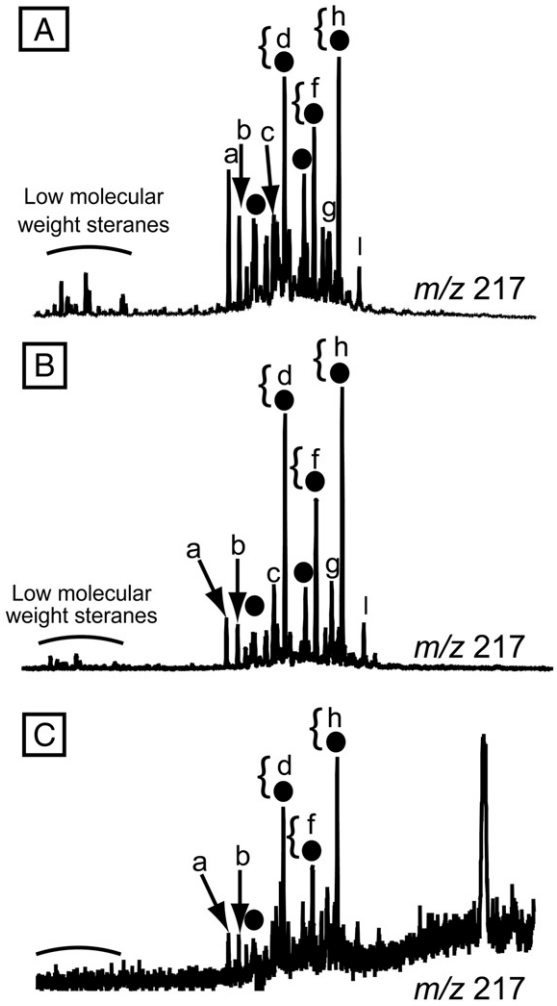

Fig. 7. Distribution of steranes highlighted by partial *m*/*z* 217 mass chromatograms of the saturated hydrocarbons extracted from mud breccia sediments from [A] Captain Arutyunov MV (GeoB9072); [B] Bonjardim MV (AT624); [C] Olenin MV (AT626). Partial total ion current mass chromatograms are shown in Fig. 5. The key to compound identification is provided in Table 4.

C_3H_8) ratios (Fig. 2a; Tables 2 and 3). Samples from Porto, Semenovich, and Soloviev MVs are highly enriched in CH_4, whereas gases from Bonjardim, Olenin and Carlos Ribeiro MVs have low $CH_4/(C_2H_6 + C_3H_8)$ ratios. On the Moroccan margin, gases vented at Meknes MV, CAMV and two locations at Ginsburg MV (cores AT521 and AT522) are also highly enriched in CH_4 and have the same isotopic composition (Table 2 and Fig. 2). The variation in the distribution of hydrocarbons is unlikely to result from mixing of microbial and thermogenic gas sources because rates of shallow microbial methanogenic activity are very low in Gulf of Cadiz MV sediments (Nuzzo et al., 2008) and because changes in the molecular distribution do not correlate to changes in $\delta^{13}C$–CH_4 values (Fig. 2a). Consistently, δ^2H–CH_4 values ~−200‰ at all sites except for Porto MV suggest a common origin for CH_4 as shown on the "CD" diagram in Fig. 2b, which is an empirical guide that can be used to distinguish CH_4 formed by thermal cracking of *n*-alkanes versus that formed by methanogenic *Archaea* oxidizing H_2 coupled to the reduction of CO_2 or dissimilating acetic acid (Whiticar et al., 1986).

5.1.2. Archaeal methane at Porto MV?

At Porto MV, the gases are highly enriched in CH_4 having $\delta^{13}C$ values ranging from ~−55 to −50‰ as at all the sites mentioned above, but distinctively more negative δ^2H–CH_4 values of −267 to −253‰ which are indicative of an aceticlastic Archaeal origin (Fig. 2b). Methane formed by acetate fermentation is ^{13}C-enriched compared to other Archaeal sources because carbon isotope fractionation between the methyl group of acetate (substrate) and methane (product) is small (as little as 7‰) for thermophilic organisms (Valentine et al., 2004). Methane vented and trapped in clathrates at Porto MV could be produced mainly by aceticlastic methanogens in the deep sediments, although $\delta^{13}C$–CH_4 values are similar to those of typical thermogenic CH_4 at Gulf of Cadiz MVs. A shallow microbial origin for the gas can probably be excluded because of the low Total Organic Carbon content of ~0.3 wt.% of Porto MV mud breccia sediments. Notably, pore water acetate concentrations of up to 2478 ± 163 μM have been measured at Ginsburg MV (Nuzzo et al., 2008), which shows that deep-sourced fluids at Gulf of Cadiz MVs can be very highly enriched in organic acids, although such measurements have not been performed at Porto MV. At Ginsburg MV, the deep-sourced fluid is also enriched in sulphate, and the high levels of acetate do not stimulate methanogenesis but instead are oxidized to CO_2 coupled to the reduction of SO_4^{2-} (Nuzzo et al., 2008). The pore fluids are not enriched in sulphate at Porto MV, and consequently the

presence of acetate in the interstitial fluids could fuel methanogenic activity. Methane production by *Archaea* fermenting acetate supplied by deep-sourced fluids could occur at depth in the buried sediments or in shallow extruded sediments.

5.1.3. "Mature thermogenic gases": Ginsburg and Mercator MVs

The pore water gases from the active vent at Mercator MV (MSM1-239) contain CH_4 that is more ^{13}C- and ^{2}H-enriched than CH_4 from the non-active location at the same MV (MSM1-263; Fig. 2), This indicates that CH_4 vented at the bubbling site (MSM1-239) has a higher formation temperature because residual CH_4 becomes further enriched in heavy isotopes for both C and H during late maturation stages due to an open system Raleigh distillation effect occurring throughout the thermal maturation process (Schoell, 1980). A high maturity thermogenic origin also is consistent with the limited differences in carbon isotopic composition between the homologues in samples from site MSM1-239 at Mercator MV (Fig. 3) because these differences are known to decrease during the maturation process (James, 1983). The gas from core GeoB9061 at Ginsburg MV has the same isotopic and molecular composition as gas in core MSM1-263 at Mercator MV (Fig. 2). Samples from both cores plot along a mixing line between low thermal maturity gases (e.g., Bonjardim and Carlos Ribeiro MVs) and high maturity gas from the active Mercator MV vent (core MSM1-239) in the Bernard and CD diagrams, suggesting that they are probably produced by mixing of gases from both sources (Fig. 2). This hypothesis is supported by the molecular and isotopic compositions of gases sampled from cores AT521 and AT522 at Ginsburg MV, which are typical of the lower thermal maturity gases vented at CAMV, Meknes MV or at the DPF MVs. We therefore propose that mixtures of thermogenic gases of different thermal maturities (i.e., sources) are vented at different locations of Ginsburg and Mercator MVs.

5.2. Effects of transport and biodegradation in the shallow sub-surface on hydrocarbon gas composition

The deep-source thermogenic hydrocarbon gases vented at all Gulf of Cadiz MVs have experienced extensive transport, and during transport in solution, different hydrocarbon gas homologues can become separated because their solubility in water increases with increasing molecular weight (McAullife, 1966). This separation process results in a progressive enrichment in the lighter homologues, predominantly CH_4. The diffusion of CH_4 in the sediments has been found to have no influence on its isotopic composition according to some authors (Fuex, 1980), and on the contrary to induce a progressive depletion in ^{13}C, with differences in $\delta^{13}C$ values between source and migrated CH_4 of 20‰ or more (Prinzhofer and Pernaton, 1997). Hence the enrichment in CH_4 relative to its heavier homologues at many "lower thermal maturity" sites could be produced by a transport effect inducing (i) changes in CH_4/C_{2+} ratios but no marked changes in $\delta^{13}C$ values (i.e. $\delta^{13}C$–CH_4 of source gas ~−50‰) or (ii) changes both in the molecular composition of the migrated gas and in $\delta^{13}C$–CH_4 values (i.e. $\delta^{13}C$–CH_4 of source gas < −50‰). In either case, the effects of transport on the molecular composition of light volatile hydrocarbon gases can account for the varying CH_4/C_{2+} ratios at "lower thermal maturity" sites.

Biodegradation of thermogenic gases also can alter their composition; C_3H_8, *n*-C_4H_{10} and *n*-C_5H_{12} are more extensively degraded than their branched homologues, leading to ^{13}C-enrichment in residual gas compared to undegraded gas (James and Burns, 1984). No clear trend for decreasing pore water C_3H_8 concentrations coupled to increasing $\delta^{13}C$–C_3H_8 values can be seen at Gulf of Cadiz MVs, except for a few data points at CAMV (core MSM1-174) where low concentrations of ^{13}C-enriched propane indicate extensive biodegradation processes have taken place, Carlos Ribeiro MV (core AT613) and Mercator MV (Fig. 4a). In core AT613 at Carlos Ribeiro MV, an increase in the *i*-C_4H_{10}/*n*-C_4H_{10} ratio coincides with an increase in $\delta^{13}C$-*n*-C_4H_{10} values, suggesting that *n*-butane has been biodegraded (Fig. 4b). At this site, low $\delta^{13}C$ values for CH_4 and C_2H_6 (Fig. 3) also suggest the occurrence of microbial generation of CH_4 and C_2H_6 (e.g., Milkov et al., 2005). Hence at Carlos Ribeiro MV and CAMV, biodegradation of propane and *n*-butane, as well as secondary methane and ethane production at Carlos Ribeiro MV partly explain variations in gas geochemistry in samples from different cores. However, our results exclude the hypothesis of significant biodegradation processes at all other MVs, and the large range of CH_4/C_{2+} ratios observed at low thermal maturity sites are best explained by extensive transport effects.

5.3. Petroleum in sediments from Gulf of Cadiz MVs

5.3.1. Mixed sources of organic matter in mud volcano sediments

The distribution of selected lipid biomarkers indicates that there are multiple sources of organic matter having different thermal maturities and that the proportional abundance of immature versus mature organic matter varies amongst the sites. The distribution of *n*-alkanes at Olenin MV is marked by the predominance of odd-numbered homologues in the range of C_{25} to C_{31} and a correspondingly high CPI, the later being characteristic of thermally immature organic matter dominated by a significant contribution from terrestrial plants (e.g. Eglington and Hamilton, 1967; Fig. 5 and Table 5). Further evidence that extractable organic matter at the Olenin MV is thermally immature comes from the predominance of the biogenic, but thermodynamically unfavourable ββ configuration of the hopanes (Fig. 6 and Table 5). On the contrary, the *n*-alkane distribution at CAMV (Fig. 5a and Table 5) is dominated by relatively low molecular weight homologues with no odd-over-even predominance (reflected by a CPI of ~1) and abundant pristane and phytane. Such a composition is typical for thermally mature organic matter, whether petroleum (i.e., migrated out of the source rock) or bitumen (i.e., immobile phase in the source rock). Further evidence that this organic matter is thermally mature is the homohopane isomerization ratio (22S/(22R + 22S)), which is approximately 0.6 and typical of bitumen that has reached at east the oil window (e.g., Seifert and Moldowan, 1986; Table 5). It is also in agreement with an elevated monoaromatic steroid ratio (MA(I)/[MA(I) + MA(II)]) value of 50% (e.g., Seifert and Moldowan, 1978), low βα/(βα + αβ) norhopane ratios and the most elevated diasterane/(diasterane + sterane) ratios of all sites (Peters et al., 1990).

CPIs from other MVs show intermediate values, reflecting contributions from both the petroleum/bitumen and higher plant-derived patterns, with a predominance of thermally mature organic matter at Carlos Ribeiro, Semenovich and Bonjardim MVs, and low maturity organic matter at Ginsburg and Porto MVs (Table 5). Supporting a mixed source of organic matter, the biomarker thermal maturity parameters at the Semenovich, Bonjardim, Porto, Ginsburg, and Shouen MVs are intermediate between the CAMV and Olenin MV end-members. The parameters listed in Table 5 suggest that the thermal maturity of bitumen at the sites decreases in the order CAMV > Carlos Ribeiro MV > Semenovich MV > Ginsburg MV > Porto MV, with organic matter at Olenin MV containing only thermally immature organic matter. However, both 17β,21β(H) hopanes (immature) and 17α,21β(H)-homohopanes with a 22S/(22S + 22R) ratio of 0.6 (mature) are present at CAMV. Likewise, the occurrence of thermally mature and immature biomarkers is observed at all other sites (Table 5). Thus the distribution of hydrocarbons suggests that thermally immature organic matter from the sediment is mixed with varying proportions of petroleum that has migrated upward into shallow sediments. This implies that a relatively shallow mud source, which has experienced little thermal maturation, has been fluidized by the influx of deep fluids (Hensen et al., 2007), associated not only with hydrocarbon gases but also with petroleum.

5.3.2. Thermal maturity and the origin of petroleum at Gulf Of Cadiz MVs

The thermal maturity of the petroleum transported from depth into the shallow mud source can be inferred from the parameters listed in Table 5. At no site does the organic matter of inferred petroleum origin exceed an equivalent temperature range ~100 °C because higher temperatures would begin to cause thermal degradation of steranes and hopanes (Peters and Moldowan, 1991). Such temperatures are consistent with the range of diasterane and monoaromatic steroid ratios (Peters et al., 1990). Positive heat flux anomalies are rare over most of the Gulf of Cadiz, being observed only in the West in the area of Porto, Bonjardim and Carlos Ribeiro MVs (Kopf et al., 2004; Grevemeyer et al., 2009). Therefore the petroleum transported from depth into the shallower mud breccia source is probably formed at depths <3–4 km, well within the mixed terrestrial and marine Mio-Pliocene sediments (Medialdea et al., 2004). Mixed sedimentary sources are also in agreement with the C_{27} to C_{29} sterane distributions which suggest a mixed terrestrial and marine sedimentary source rock (Table 5). Both petroleum sources and generation temperatures (~60–100 °C) correspond to those expected for the generation of high amounts of clay-dehydration fluids across the wedge (Hensen et al., 2007).

5.4. Conclusion: Tectonic and stratigraphic control on the generation and transport of hydrocarbon gases at Gulf of Cadiz MVs

The Gulf of Cadiz MVs have previously been divided into two groups based on the molecular and isotopic composition of the light volatile hydrocarbon gases: the Moroccan Margin (high thermal maturity) and DPF (lower thermal maturity) sites (Stadnitskaia et al., 2006). Our findings support a predominantly thermogenic origin for gases vented at MVs across the Gulf of Cadiz, but indicate that there is not a common source for each of the groups defined by Stadnitskaia et al. (2006), but rather a higher variety of cases in which local tectonic and stratigraphic conditions control both hydrocarbon formation and transport mechanisms. The differences in molecular and isotopic compositions between the 11 sites investigated across the Gulf of Cadiz are mainly attributed to their generation in distinct stratigraphic and tectonic settings, as exemplified by Mercator MV, CAMV, Bonjardim MV and Porto MV. The dominant gas production and transport processes at the other sites investigated in this study are related to those of the four models presented below.

5.4.1. Evaporitic deposits in the sediments: admixing of thermogenic gases from different depths (Mercator and Ginsburg MVs)

At Mercator MV ("high thermal maturity" site), the sulphate concentrations in the deep-sourced fluid exceed saturation values, suggesting the presence of thick gypsum-bearing evaporitic deposits at depth (Haeckel et al., 2007), which is supported by geophysical data for this area (Flinch, 1996). The presence of evaporites also is suspected at Ginsburg MV (Hensen et al., 2007). It is thus likely that the evaporites act as a barrier between deeper and shallower hydrocarbon-bearing sediments, with metagenic CH_4 production occurring in the deepest compartment and lower maturity gases in the upper sediments. Additionally, the availability of sulphate in deep interstitial fluids may promote the anaerobic oxidation of hydrocarbons at depth. Although it is unlikely that deep thermal or microbial oxidation of methane is solely responsible for the increased $\delta^{13}C$–CH_4 values at the active seep (Barker and Fritz, 1981; Krouse et al., 1988) because the sulphate concentrations are high in pore fluids at both Mercator MV locations (as opposed to only at the active vent), both thermal maturation and anaerobic oxidation result in increasing $\delta^{13}C$–CH_4 and $\delta^{2}H$–CH_4 values and can explain the values observed at this site. The processes of transport and mixing of hydrocarbon gases are schematically depicted for Mercator MV in

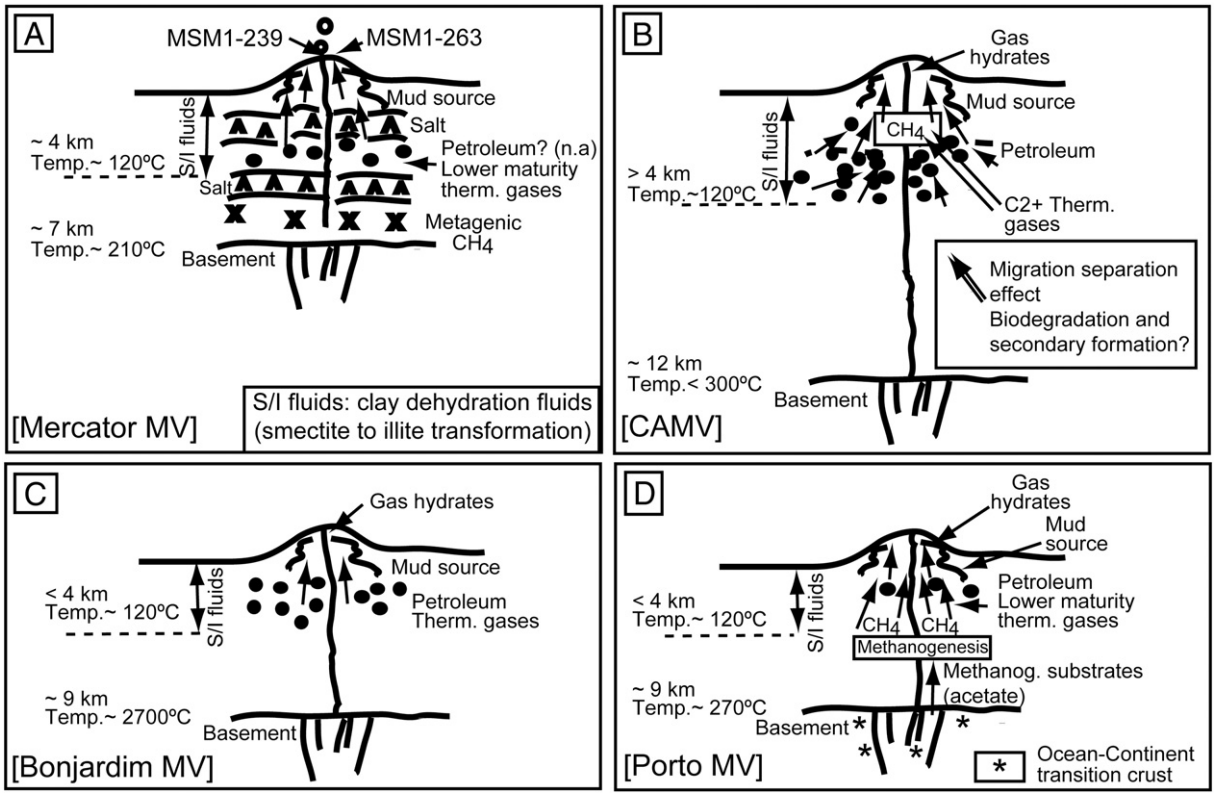

Fig. 8. Schematic representation of the sources and transport mechanisms for hydrocarbon gases, fluids, petroleum and mud at [A] Mercator MV; [B] CAMV; [C] Bonjardim MV; and [D] Porto MV. See explanations in the text. Basement depths from Thiebot and Gutscher, 2006.

Fig. 8a. Clay mineral fluid expulsion and thermogenic gas formation occur to a depth of ~4 km, with further cracking of homologues to methane (metagenesis), and possibly AOM, occurring beneath salt deposits at greater depths (Fig. 8a). Transport and mixing of the metagenic CH_4 and lower thermogenic hydrocarbon gases are favoured by the location of the MV along a major south west iberian margin strike–slip fault (Zitellini et al., 2009; "SWIM" fault in Fig. 1) as observed at other MVs from the Gulf of Cadiz (Hensen et al., 2007) and from other settings (e.g., Mediterranean Ridge: Huguen et al., 2004). In the conceptual model presented here, gas vented at the bubbling site (core MSM1-239) contains essentially deeper-sourced CH_4, while at the other location (MSM1-263) it is produced by mixing of gases from deep and shallow sources (Fig. 8a). We propose that similar processes are occurring at Ginsburg MV.

5.4.2. Extensive generation and transport of fluids, petroleum and hydrocarbon gases from deeply-buried sediments (Captain Arutyunov, Meknes, Semenovitch and Soloviev MVs)

CAMV is also located on the Moroccan Margin, but in an area where sediment thickness is greater than anywhere else in the Gulf of Cadiz (up to 14 km; Thiebot and Gutscher, 2006). Although evaporitic deposits are probably present at CAMV, pore fluid geochemical studies show that their occurrence is much more limited than at Mercator or Ginsburg MVs (Hensen et al., 2007). We propose that the enhanced flux of deep-sourced clay mineral dehydration fluid (Hensen et al., 2007), hydrocarbon gases and petroleum in shallow sediments from CAMV results from a combination of (i) the generation of greater volumes of fluids and hydrocarbons, and (ii) increased rates of transport due to the location of the MV at the tip of a major lateral fault (Fig. 1; Hensen et al., 2007).

The production of large amounts of fluid, oil and hydrocarbon gases is attributed to both the thickness of the sediments and the low thermal gradient in this part of the wedge (Kopf et al., 2004; Grevemeyer et al., 2009), which together allow for generation to take place at ~60–100 °C over greater depth intervals. Extensive migration of thermogenic gases is also consistent with increased thickness of the sediments in this area and could account for the higher CH_4/C_{2+} ratios at CAMV than at Carlos Ribeiro and Bonjardim MVs. The influx of fluids and gases drives the mobilization of shallow mud sources, and immature organic matter from the mobilized sediments is mixed with petroleum that has migrated along with the gases, as depicted in Fig. 8b.

The upward-directed transport of deep-sourced fluids and hydrocarbons is favoured by the location of CAMV at the tip of a wide lateral fault (Figs. 1 and 8b), as indicated by increased advection rates of upward-transported fluids at this site (Hensen et al., 2007). We tentatively propose that Meknes, Semenovich and Soloviev MVs have analogous functioning because of the similarity in geochemical composition of gases, sediments and fluids (Nuzzo, 2007), and tectonic settings. These structures are indeed located on recently-discovered "SWIM" lateral faults (Zitellini et al., 2009; Fig. 1), similar to CAMV.

5.4.3. Active generation of C_{2+} - enriched gases under tectonic control (Carlos Ribeiro, Bonjardim and Olenin MVs)

Sediment thicknesses decrease westward in the area of the DPF MVs (Thiebot and Gutscher, 2006) and evaporites are absent in this part of the wedge (Medialdea et al., 2004). NE–SW and NW–SE oriented thrust faults predominate in this area (Fig. 1) and positive heat flux anomalies have been measured across W–E transects over thrust faults (Kopf et al., 2004; Grevemeyer et al., 2009). The MVs are located at the intersection of thrust faults with regional-scale lateral faults such as the Porto–Bonjardim Fault (Fig. 1) along which both the MVs are located (Pinheiro et al., 2005). Increased heat fluxes are expected to promote the generation of clay-dehydration fluids and C_{2+}-enriched gases at shallower depths in the area of the DPF MVs (<4 km) than in the vicinity of CAMV, as schematically shown for Bonjardim MV in Fig. 8c. However, the co-occurrence of thermally immature and mature biomarkers in mud breccia sediments demonstrates that hydrocarbons (petroleum and gases) have migrated in the sediments, because the thermally unstable biomarkers would not be present if generation had taken place within the MV source sediments. Hence active thermogenic gas generation is probably controlled by the westward movement of the sedimentary prism, which is accommodated by thrust faults (Gutscher et al., 2002; Zitellini et al., 2009), independently from the processes leading to mud volcanism along major strike–slip faults (Pinheiro et al., 2005; Hensen et al., 2007). Nevertheless, the hydrocarbon gases vented at Bonjardim MV have probably experienced less extensive transport than gases vented at CAMV, as indicated by lower CH_4/C_{2+} ratios at the former site (Fig. 8). We propose that at Carlos Ribeiro and Olenin MVs C_{2+}-enriched gases are also generated at depths <4 km due to increased heat fluxes in the area. However, gases vented at Olenin MV probably have a shallower origin and thus much lower concentrations, consistent with the near absence of petroleum in Olenin MV sediments. The abundance of petroleum in Carlos Ribeiro MV sediments is higher than at Bonjardim MV (refer to CPI values; Table 5) perhaps because of the presence of higher amounts of petroleum in buried sediments from the area of Carlos Ribeiro MV than from the more distal area of Bonjardim MV.

5.4.4. Deep acetoclastic methanogenesis at Porto MV?

Porto MV is located at the toe of the active sedimentary wedge (Zitellini et al., 2009) close to the Coral Patch crustal high in an area which is probably floored by ocean–continent transition crust (OCTC in Fig. 8d; Contrucci et al., 2004). The C and H isotope composition of CH_4 are consistent with a major contribution from *Archaea* microbes, probably based upon acetate dissimilation (Whiticar et al., 1986). The small amount of oil in mud breccia sediments from Porto MV (Table 5) is also in agreement with a limited thermogenic origin of hydrocarbon gases vented at this site. However, the TOC value in Porto MV sediment is low and given the distal location of the MV, it is unlikely that the sedimentary organic matter is labile enough to sustain a significant microbial activity. Archaeal CH_4 production is instead more likely related to acetate enrichment of the deep-sourced fluids. The production of fluids enriched in reduced methanogenic substrates at depth should be investigated further because it is expected to involve the deep hydrothermal alteration of OCTC basement rocks and therefore has important implications regarding the "microbial link" between crustal and sedimentary processes.

Acknowledgements

We would like to thank the scientific staff and chief/co-chief scientists of the *RV-Sonne* SO175-2, *RV-Merian* MSM1, and *RV-Professor Logachev* TTR cruises: Prof. Achim Kopf (University of Bremen, Germany), Prof. Olaf Pfannkuche (IFM-GEOMAR, University of Kiel, Germany) and Prof. Michael Ivanov (Moscow State University, Russia), respectively. We are very grateful to Ian Bull and Rob Berstan of the NERC Life Sciences Mass Spectrometry Facility (Bristol node) for assistance with biomarker and GC-C-IRMS analyses. We are indebted to Mark Schmidt for his insightful comments on an early version of this work, and to John Pohlman and an anonymous reviewer for providing very thorough reviews that have greatly improved this manuscript. This work was performed while MN benefited from a PhD grant from the Fundação para a Ciência e a Tecnologia (Portugal), and was further supported by the MVSEIS-Euromargins (01-LEC-EMA24F; PDCTM72003/DIV/40018) and EU-METROL ESF-funded projects as well as by the Sonderforschungsbereich 574 at Christian-Albrechts-Universität, Kiel (SFB publication no. 103), the R&D programme GEOTECHNOLOGIEN funded by the German Ministry of Education and

Research (BMBF) and the German Research Council (DFG), grant 03G0600D.

References

Argus, D.F., Gordon, R.G., Demets, C., Stein, S., 1989. Closure of the Africa–Eurasia–North America plate motion circuit and tectonics of the Gloria fault. Journal of Geophysical Research 94, 5585–5602.

Barker, J., Fritz, P., 1981. Carbon isotope fractionation during microbial methane oxidation. Nature 293, 289–291.

Bernard, B.B., Brooks, J.M., Sackett, W.M., 1978. Light hydrocarbons in recent Texas continental shelf and slope sediments. Journal of Geophysical Research 83, 4053–4061.

Blinova, V.N., Ivanov, M.K., Böhrmann, G., 2003. Hydrocarbon gases in deposits from mud volcanoes in the Sorokin Trough, North-Eastern Black Sea. Geo-Marine Letters 23 (3–4), 250–257.

Bowes, H.L., Hornibrook, E.R.C., 2006. Emission of highly ^{13}C-depleted methane from an upland blanket mire. Geophysical Research Letters 33, L04401. doi:10.1029/2005GL025209.

Brown, K.M., 1990. The nature and hydrogeologic significance of mud diapirs and diatremes for accretionary systems. Journal of Geophysical Research 95 (B6), 8969–8982.

Buforn, E., Sanz de Galeano, C., Udias, A., 1995. Seismotectonics of Ibero–Maghrebian region. Tectonophysics 248, 247–261.

Charlou, J.L., Donval, J.P., Zitter, T., Roy, N., Jean-Baptiste, P., Foucher, J.P., Woodside, J., MEDINAUT Scientific Party, 2003. Evidence of methane venting and geochemistry of brines on mud volcanoes of the eastern Mediterranean Sea. Deep-Sea Research 50, 941–958.

Chung, H.M., Gormly, J.R., Squires, R.M., 1988. Origin of gaseous hydrocarbons in subsurface environments: theoretical considerations of carbon isotope distribution. Chemical Geology 71, 97–103.

Contrucci, I., Klingelhöfer, F., Perrot, J., Bartolomé, R., Gutscher, M.-A., Sahabi, M., Malod, J., Rehault, J.-P., 2004. The crustal structure of the NW Moroccan continental margin from wide-angle and reflection seismic data. Geophysical Research International 159, 117–128.

Coplen, T.B., 2008. Explanatory glossary of terms used in expression of relative isotope ratios and gas ratios (IUPAC Recommendations 2008. International Union of Pure and Applied Chemistry, pp. 1–27.

Diaz-del-Rio, V., Somoza, L., Martinez-Frias, J., Mata, J.P., Delgado, A., Hernandez-Molina, F.J., Lunar, R., Martin-Rubi, J.A., Maestro, A., Fernandez-Puga, M.C., Leon, R., Llave, E., Medialdea, T., Vasquez, J.T., 2003. Vast fields of hydrocarbon-derived carbonate chimneys related to the accretionary wedge/olistostrome of the Gulf of Cadiz. Marine Geology 195, 177–200.

Eglington, G., Hamilton, R.J., 1967. Leaf epicutilar waxes. Science 156, 1322–1335.

Flinch, J.F., 1996. Accretion and extensional collapse of the external western Rif (Northern Morocco). In: Zeigler, P.A.H., F. (Eds.), Peri Tethys Memoir 2: Structure and prospects of Alpine basins and Forelands, vol. 170, pp. 61–85.

Fuex, A.N., 1980. Experimental evidence against an appreciable isotopic fractionation of methane during migration. In: Douglas, E.M., Maxwell, J.R. (Eds.), Advances in Organic Geochemistry, 1979. Pergamon, pp. 639–646.

Gràcia, E., Dañobeitia, J., Verges, J., Bartolomé, R., 2003a. Crustal architecture and tectonic evolution of the Gulf of Cadiz (SW Iberian margin) at the convergence of the Eurasian and African plates. Tectonics 22 (NO4), 1033. doi:10.1029/2001TC901045.

Gràcia, E., Dañobeitia, J., Verges, J., PARCIFAL, T.E.A.M., 2003b. Mapping active faults offshore Portugal (36°N–38°N): implications for seismic hazard assessment along the southwest Iberian margin. Geology 31 (1), 83–86.

Grevemeyer, I., Kaul, N., Kopf, A., 2009. Heat flow anomalies in the Gulf of Cadiz and off Cape San Vincente, Portugal. Marine and Petroleum Geology 26 (6), 795–804.

Gutscher, M.-A., Malod, J., Rehault, J.-P., Contrucci, I., Klingelhoefer, K., Mendes-Victor, L., Spakman, W., 2002. Evidence for active subduction beneath Gibraltar. Geology 30 (12), 1071–1074.

Haeckel, M., Berndt, C., Liebetrau, V., Linke, P., Reitz, A., Schoenfeld, J., Vanneste, H., 2007. Genesis and rates of fluid flow at the Mercator mud volcano, Gulf of Cadiz. Geochimica et Cosmochimica Acta 71 (15) Suppl. S, A367.

Hedberg, H.D., 1974. Relation of methane generation to undercompacted shales, shale diapirs, and mud volcanoes. American Association of Petroleum Geologists Bulletin 58 (4), 661–673.

Hensen, C., Nuzzo, M., Hornibrook, E.R.C., Pinheiro, L.M., Bock, F., Magalhães, V.H., Brückmann, W., 2007. Sources of mud volcano fluids in the Gulf of Cadiz — indications for hydrothermal imprint. Geochimica et Cosmochimica Acta 71, 1232–1248.

Horita, J., Berndt, M., 1999. Abiogenic methane formation and isotopic fractionation under hydrothermal conditions. Science 285, 1055–1057.

Huguen, C., Mascle, J., Chaumillon, E., Kopf, A., Woodside, J., Zitter, T., 2004. Structural setting and tectonic control of mud volcanoes from the Central Mediterranean Ridge (Eastern Mediterranean). Marine Geology 209, 245–263.

James, A.T., 1983. Correlation of natural gas by use of carbon isotopic distribution between hydrocarbon components. American Association of Petroleum Geologists Bulletin 67 (7), 1176–1191.

James, A.T., Burns, B.J., 1984. Microbial alteration of subsurface natural gas accumulations. American Association of Petroleum Geologists Bulletin 68 (8), 957–960.

Kenyon, N.H., Ivanov, M.K., Akhmetzhanov, A.M., Akhmanov, G.G., 2005. Interdisciplinary Geoscience Research on the NorthEast Atlantic Margin, Mediterranean Sea and Mid-Atlantic Ridge. Preliminary Results of Investigations During the TTR-13 Cruise of RV Professor Logachev June–August, 2003. United Nations Educational, Scientific and Cultural Organization, Paris.

Kopf, A., Bannert, B., Brückmann, W., Dorschel, B., Foubert, A.T.G., Grevemeyer, I., Gutscher, M.-A., Hebbeln, D., Heesemann, B., Hensen, C., Kaul, N.E., Lutz, M., Magalhães, V.H., Marquardt, M.J., Marti, A.V., Nass, K.S., Neubert, N., Niemann, H., Nuzzo, M., Poort, J.P.D., Rosiak, U.D., Sahling, H., Schneider von Deimling, J., Somoza, L.L., Thiebot, E., Wilkop, T. P., 2004. Report and preliminary results of Sonne Cruise SO175. MIAMI - BREMERHAVEN, 12.11 – 30.12.2003. Berichte, Fachbereich Geowissenschaften, Universität Bremen, No. 228, p. 218.

Krouse, H.R., Viau, C.A., Eliuk, L.S., Ueda, A., Halas, S., 1988. Chemical and isotopic evidence of thermochemical sulphate reduction by light hydrocarbon gases in deep carbonate reservoirs. Nature 333, 415–419.

Lonergan, L., White, N., 1997. Origin of the Betic-Rif mountain belt. Tectonics 16 (3), 504–522.

Mastalerz, V., de Lange, G., Dählmann, A., Feseker, T., 2007. Active venting at Isis mud volcano, offshore Egypt: origin and migration of 2 hydrocarbons. Chemical Geology 246, 87–106.

Mazurenko, L.L., Belenkaya, I., Ivanov, M.K., Pinheiro, L.M., 2002. Mud volcano gas hydrates in the Gulf of Cadiz. Terra Nova 14 (5), 321–329.

Mazurenko, L.L., Soloviev, V.A., Gardner, J.M., Ivanov, M.K., 2003. Gas hydrates in the Ginsburg and Yuma mud volcano sediments (Moroccan Margin): results of chemical and isotopic studies of pore water. Marine Geology 195 (1–4), 201–210.

McAullife, C., 1966. Solubility in water of paraffin, cycloparaffin, olefin, acetylene, cycloolefins and aromatic hydrocarbons. Journal of Physical Chemistry 70, 1267–1275.

McAullife, C., 1971. GC determination of solutes by multiple phase equilibration. Chemie & Techniek 1, 46–51.

McCollom, T.M., Seewald, J.S., 2006. Carbon isotope composition of organic compounds produced by abiotic synthesis under hydrothermal conditions. Earth and Planetary Science Letters 243, 74–84.

Medialdea, T., Vegas, R., Somoza, L., Vazquez, J.T., Maldonaldo, A., Diaz-del-Rio, V., Maestro, A., Cordoba, D., Fernandez-Puga, M.C., 2004. Structure and evolution of the 'olistostrome' complex of the Gibraltar Arc in the Gulf of Cadiz (eastern Central Atlantic): evidence from two long seismic cross-sections. Marine Geology 209, 173–198.

Milkov, A.V., 2005. Molecular and stable isotope composition of natural gas hydrates: a revised global dataset and basic interpretations in the context of geological settings. Organic Geochemistry 36, 681–702.

Milkov, A.V., Claypool, G.E., Lee, Y.-J., Sassen, R., 2005. Gas hydrate systems at Hydrate Ridge offshore Oregon inferred from molecular and isotopic properties of hydrate-bound and void-gases. Geochimica et Cosmochimica Acta 69 (4), 1007–1026.

Niemann, H., Duarte, J., Hensen, C., Omoregie, E., Magalhães, V.H., Elvert, M., Pinheiro, L.M., Kopf, A., Boetius, A., 2006. Microbial methane turnover at mud volcanoes of the Gulf of Cadiz. Geochimica et Cosmochimica Acta 70, 5336–5355.

Nuzzo, M. 2007. The origin of light volatile hydrocarbon gases in mud volcanoes, Gulf of Cadiz. PhD. Thesis, University of Bristol (UK), 350p.

Nuzzo, M., Hornibrook, E.R.C., Hensen, C., Parkes, R.J., Cragg, B.A., Rinna, J., Schneider von Deimling, J., Sommer, S., Magalhães, V.H., Reitz, A., Brückmann, W., Pinheiro, L.M., 2008. Shallow microbial recycling of deep-sourced carbon in Gulf of Cadiz mud volcanoes. Geomicrobiology Journal 25, 283–295.

Peters, K.E., Moldowan, J.M., 1991. Effects of source, thermal maturity and biodegradation on the distribution and isomerization of homohopanes in petroleum. Organic Geochemistry 17, 47–61.

Peters, K.E., Moldowan, J.M., Sundararaman, P., 1990. Effects of hydrous pyrolysis on biomarker thermal maturity parameters: Monterey phosphatic and siliceous members. Organic Geochemistry 15, 249–265.

Pinheiro, L.M., Ivanov, M.K., Sautkin, A., Akhmanov, G., Magalhães, V.H., Volkonskaya, A., Monteiro, J.H., Somoza, L., Gardner, J., Hamouni, N., Cunha, M.R., 2003. Mud volcanism in the Gulf of Cadiz: results from the TTR-10 cruise. Marine Geology 195, 131–151.

Pinheiro, L.M., Ivanov, M., Kenyon, N., Magalhães, V., Somoza, L., Gardner, J., Kopf, A., Rensbergen, P.V., Monteiro, J.H., Team, Euromargins-MVSEIS, 2005. Structural control of mud volcanism and hydrocarbon-rich fluid seepage in the gulf of Cadiz: Recent results from the TTR-15 cruise. CIESM Research Workshop, Fluid Seepages/Mud Volcanoes in the Mediterranean and Adjacent Domains.

Prinzhofer, A., Pernaton, E., 1997. Isotopically light methane in natural gas: bacterial imprint or diffusive fractionation? Chemical Geology 142, 193–200.

Sartori, R., Torelli, L., Zitellini, N., Peis, D., Lodolo, E., 1994. Eastern segment of the Azores–Gibraltar line (Central-Eastern Atlantic): an oceanic plate boundary with diffuse compressional deformation. Geology 22, 555–558.

Schmidt, M., Hensen, C., Morz, T., Muller, C., Grevemeyer, I., Wallmann, K., Mau, S., Kaul, N., 2005. Methane hydrate accumulation in "Mound 11" mud volcano, Costa Rica forearc. Marine Geology 216 (1–2), 83–100.

Schoell, M., 1980. The hydrogen and carbon isotopic composition of methane from natural gases of various origins. Geochimica et Cosmochimica Acta 44, 649–661.

Seifert, W.K., Moldowan, J.M., 1978. Applications of steranes, terpanes and monoaromatics to the maturation, migration and source of crude oils. Geochimica et Cosmochimica Acta 42, 77–95.

Seifert, W.K., Moldowan, J.M., 1986. Use of biological markers in petroleum exploration. In: Johns, R.B. (Ed.), Methods in Geochemistry and Geophysics, vol. 24, pp. 261–290.

Stadnitskaia, A., Ivanov, M.K., Blinova, V., Kreulen, R., van Weering, T.C.E., 2006. Molecular and isotopic variability of hydrocarbon gases from mud volcanoes in the Gulf of Cadiz, NE Atlantic. Marine and Petroleum Geology 23, 281–296.

Stadnitskaia, A., Ivanov, M.K., Sinninghe Damsté, J.S., 2008. Application of lipid biomarkers to detect sources of organic matter in mud volcano deposits and post-eruptional methanotrophic processes in the Gulf of Cadiz, NE Atlantic. Marine Geology 225 (1–2), 1–14.

Thiebot, E., Gutscher, M.-A., 2006. The Gibraltar Arc seismogenic zone (part 1): constraints on a shallow east dipping fault plane source for the 1755 Lisbon earthquake provided by seismic data, gravity and thermal modeling. Tectonophysics 426 (1–2), 135–152.

Valentine, D.L., Chidthaisong, A., Rice, A., Reeburgh, W.S., Tyler, S.C., 2004. Carbon and hydrogen isotope fractionation by moderately thermophilic methanogens. Geochimica et Cosmochimica Acta 68 (7), 1571–1590.

Van Rooij, D., Depreiter, D., Bouimetarham, I., de Boever, E., Rycker, K.D., Foubert, A., Huvenne, V., Reveillaud, J., Staelens, P., Verseeg, W., Henriet, J.-P., 2005. First sighting of active fluid venting in the Gulf of Cadiz. EOS Transaction of the AGU 86 (49), 509.

Whiticar, M.J., Faber, E., Schoell, M., 1986. Biogenic methane formation in marine and freshwater environments: CO_2 reduction vs. acetate fermentation-Isotope evidence. Geochimica et Cosmochimica Acta 50, 693–709.

Zitellini, N., Gràcia, E., Matias, L.M., Terrinha, P., Abreu, M.A., Alteriis, G.D., Henriet, J.-P., Dañobeitia, J., Masson, D.G., Mulder, T., Ramella, R., Somoza, L., Diez, S., 2009. The quest for the Africa–Eurasia plate boundary West of the Strait of Gibraltar. Earth and Planetary Science Letters 280 (1–4), 13–50.